© 2015. Published by The Company of Biologists Ltd | Development (2015) 142, 2810-2821 doi:10.1242/dev.123091

RESEARCH ARTICLE

Neurog1 can partially substitute for *Atoh1* function in hair cell differentiation and maintenance during organ of Corti development

Israt Jahan*, Ning Pan, Jennifer Kersigo and Bernd Fritzsch*

ABSTRACT

Atoh1, a basic helix-loop-helix (bHLH) transcription factor (TF), is essential for the differentiation of hair cells (HCs), mechanotransducers that convert sound into auditory signals in the mammalian organ of Corti (OC). Previous work demonstrated that replacing mouse *Atoh1* with the fly ortholog *atonal* rescues HC differentiation, indicating functional replacement by other bHLH genes. However, replacing *Atoh1* with *Neurog1* resulted in reduced HC differentiation compared with transient *Atoh1* expression in a 'self-terminating' *Atoh1* conditional null mouse (*Atoh1-Cre; Atoh1*$^{f/f}$). We now show that combining *Neurog1* in one allele with removal of floxed *Atoh1* in a self-terminating conditional mutant (*Atoh1-Cre; Atoh1*$^{f/kiNeurog1}$) mouse results in significantly more differentiated inner HCs and outer HCs that have a prolonged longevity of 9 months compared with *Atoh1* self-terminating littermates. Stereocilia bundles are partially disorganized, disoriented and not HC type specific. Replacement of *Atoh1* with *Neurog1* maintains limited expression of *Pou4f3* and *Barhl1* and rescues HCs quantitatively, but not qualitatively. OC patterning and supporting cell differentiation are also partially disrupted. Diffusible factors involved in patterning are reduced (*Fgf8*) and factors involved in cell-cell interactions are affected (*Jag1*, *Hes5*). Despite the presence of many HCs with stereocilia these mice are deaf, possibly owing to HC and OC patterning defects. This study provides a novel approach to disrupt OC development through modulating the HC-specific intracellular TF network. The resulting disorganized OC indicates that normally differentiated HCs act as 'self-organizers' for OC development and that *Atoh1* plays a crucial role to initiate HC stereocilia differentiation independently of HC viability.

KEY WORDS: Hair cells, Survival, Basic helix-loop-helix, Transcription factors, Misexpression, Knock-in

INTRODUCTION

Neurosensory development requires the sequential, coordinated activation and cross-regulation of numerous transcription factors (TFs) to define precursors and initiate differentiation of the various cell types of the nervous and sensory system (Fritzsch et al., 2015; Imayoshi and Kageyama, 2014; Reiprich and Wegner, 2015). Molecularly dissecting these interactions requires model systems with limited cellular diversity and stereotyped cellular patterning. The organ of Corti (OC) is such a model system, with hair cells (HCs) and supporting cells (SCs) organized into the most stereotyped cell assembly of vertebrates (Slepecky, 1996), and is suited to detect minute aberrations (Jahan et al., 2013). The stereotyped cellular pattern may allow the molecular dissection of the intricate interaction of multiple basic helix-loop-helix (bHLH) proteins (Benito-Gonzalez and Doetzlhofer, 2014; Fritzsch et al., 2010b) to define HCs/SCs.

Targeted deletion studies in mice have demonstrated that three bHLH TFs (*Neurog1*, *Neurod1*, *Atoh1*) are essential to differentiate neurons and HCs of the inner ear (Bermingham et al., 1999; Fritzsch et al., 2006, 2010b). These loss-of-function analyses also revealed cross-regulation among these bHLH TFs. For example, *Neurog1* null mice showed loss of HCs (Ma et al., 2000; Matei et al., 2005), apparently through alteration of *Atoh1* expression (Raft et al., 2007). Absence of *Neurog1* reduced HCs, whereas absence of *Neurod1* resulted in ectopic HCs in ganglia (Jahan et al., 2013). Changes in *Atoh1* expression may be mediated through cross-regulation of *Neurod1* downstream of *Neurog1* (Jahan et al., 2010). *Neurod1*, in turn, may suppress *Atoh1* in the ear (Jahan et al., 2013), comparable to its role in the cerebellum (Pan et al., 2009).

Other loss-of-function studies showed that *Atoh1* drives HC differentiation (Bermingham et al., 1999; Fritzsch et al., 2005; Pan et al., 2011), and overexpression of *Atoh1* transformed non-sensory cells into HCs (Kelly et al., 2012; Zheng and Gao, 2000). *Atoh1* differentiates HCs in the ear, and the level and duration of *Atoh1* expression regulate different types of HCs and their viability (Jahan et al., 2013; Sheykholeslami et al., 2013). Consistent with these data, self-terminating *Atoh1* (*Atoh1-Cre; Atoh1*$^{f/f}$) mice initiated near normal HC differentiation but rapidly lost most HCs by 3 weeks (Pan et al., 2012a), a loss also reported in inducible Cre lines (Cai et al., 2013; Chonko et al., 2013). Replacing both alleles of *Atoh1* with another bHLH TF, *Neurog1* (*Atoh1*$^{kiNeurog1/kiNeurog1}$), resulted in very few immature HCs bearing microvilli with a central kinocilium (Jahan et al., 2012). This inability of *Neurog1* to maintain and differentiate HCs beyond that achieved with even transient *Atoh1* expression (Pan et al., 2012a) contrasts with work on retinal ganglion cells (RGCs), in which the *Atoh1* paralog, *Atoh7*, was replaced by *Neurod1* (Mao et al., 2008). *Neurod1* can replace *Atoh7*, possibly because RGC precursors are pre-programmed to differentiate as RGCs independently of the type of bHLH TF (Mao et al., 2013). In molecular terms, the pairing of *Atoh1/Neurog1* is as different as that of *Atoh7/Neurod1* (52% versus 60% sequence similarity), suggesting that overall binding differences might not fully explain these very different results in eyes and ears. We reasoned that failure of functional replacement of *Atoh1* by *Neurog1* in the ear (Jahan et al., 2012), compared with *Atoh7* by *Neurod1* in the retina (Mao et al., 2008), or *Atoh1* by fly *atonal* (Wang et al., 2002), could relate either to 'self-regulation' of *Atoh1* via its enhancer (Helms et al., 2000) or to a unique functional requirement of Atoh1/Atonal protein to initiate HC differentiation.

To test these possibilities, we generated a new mouse model (*Atoh1-Cre; Atoh1*$^{f/kiNeurog1}$) with insertion of *Neurog1* in one allele of *Atoh1* (Jahan et al., 2012) and removal of the second floxed

Department of Biology, College of Liberal Arts & Sciences, University of Iowa, Iowa City, IA 52242, USA.

*Authors for correspondence (israt-jahan@uiowa.edu; bernd-fritzsch@uiowa.edu)

Received 10 February 2015; Accepted 13 July 2015

Development (2015) 142, 2810-2821 doi:10.1242/dev.123091

Atoh1 allele by self-termination with *Atoh1-Cre* (Pan et al., 2012a). This novel composite mouse mutant can differentiate most HCs and can rescue many HCs for up to 9 months. However, HCs stereocilia are variably disorganized, OC patterning is disrupted, and mice are deaf despite near normal numbers of rather well differentiated HCs.

RESULTS

Neurog1 expression in HCs with transient expression of *Atoh1*

We previously demonstrated that *Neurog1* replacement in both alleles of *Atoh1* resulted in expression of *Neurog1* in HC precursors that differentiate multiple microvilli (Jahan et al., 2012). Like *Atoh1* null mutant mice (Bermingham et al., 1999), homozygous *Neurog1* knock-in mice die after birth, precluding postnatal analysis. *Atoh1* autoregulates its own expression by activating an *Atoh1*-specific enhancer (Helms et al., 2000). We speculated that replacement of *Atoh1* by *Neurog1* in both alleles might have failed to activate the enhancer for adequate *Neurog1* expression under *Atoh1* promoter control (Jahan et al., 2012). To overcome this problem, we generated a novel mouse model that combined *Neurog1* knock-in in one *Atoh1* allele with a floxed second *Atoh1* allele, the latter to be excised by *Atoh1-Cre* (*Atoh1-Cre; Atoh1*$^{f/kiNeurog1}$; Fig. 1A). This newly developed *Atoh1-Cre; Atoh1*$^{f/kiNeurog1}$ model resulted in viable mice, overcoming the neonatal lethality of the homozygous *Neurog1* knock-in (Jahan et al., 2012). *Atoh1*$^{f/+}$ or *Atoh1*$^{f/f}$ mice without *Atoh1-Cre* were used as a control in this study except for the RT-qPCR analysis, where *Atoh1*$^{+/kiNeurog1}$ mice were used as control for comparison of *Neurog1* expression with *Atoh1-Cre; Atoh1*$^{f/kiNeurog1}$ mice.

In situ hybridization (ISH) showed that *Neurog1* knock-in into the *Atoh1* locus (*Atoh1-Cre; Atoh1*$^{f/kiNeurog1}$) resulted in expression of *Neurog1* in OC HCs not detected in control littermates (Fig. 1B,B′). At P0, *Atoh1-Cre; Atoh1*$^{f/kiNeurog1}$ mice showed very little *Atoh1* expression in the apex (Fig. 1C,C′). By contrast, a downstream target of *Atoh1*, *Pou4f3*, was strongly expressed in the HCs of P0 *Atoh1-Cre; Atoh1*$^{f/kiNeurog1}$ OC (Fig. 1D,D′), whereas expression of *Barhl1* was delayed compared with the vestibular epithelia at P0 (Fig. 1E,E′). At P7, qPCR showed that relative mRNA expression for *Neurog1*, *Pou4f3* and *Barhl1* in *Atoh1-Cre; Atoh1*$^{f/kiNeurog1}$ cochlea was reduced compared with *Atoh1*$^{+/kiNeurog1}$ cochlea, but the reduction was not statistically significant (*Atoh1*$^{+/kiNeurog1}$ expression was normalized to 1, Fig. 1F). In self-terminating *Atoh1-Cre; Atoh1*$^{f/f}$ mice, ISH of both *Pou4f3* and *Barhl1* showed patchy loss at P0 (Pan et al., 2012a). By contrast, *Neurog1*-misexpressing mice revealed expression of both *Pou4f3* and *Barhl1* until P7 (Fig. 1F). Partial expression of *Pou4f3* and *Barhl1* might improve HC viability, as HCs are rapidly lost in either *Pou4f3* (Hertzano et al., 2004; Xiang et al., 2003) or *Barhl1* (Li et al., 2002) null mutants.

Neurog1 misexpression with transient expression of *Atoh1* results in HC maintenance

Immunohistochemistry of Myo7a (an HC-specific marker) at P7 revealed the formation of an almost continuous row of inner hair cells (IHCs) and two to three rows of outer hair cells (OHCs) in the *Neurog1*-misexpressing mice (Fig. 2). There were occasionally two rows of IHCs. Extra rows of IHCs coincide with absence of inner pillar (IP) cells, as shown by immunohistochemistry of acetylated tubulin (which is abundant in SCs), next to the extra row of IHCs (Fig. 2B-C‴). There was no indication that the length of the cochlea was changed (supplementary material Table S1). The third row of OHCs disappeared toward the base of the cochlea, including the formation of some gaps in OHCs (Fig. 2C-D‴). Tubulin immunohistochemistry labeled differentiated IP cells, outer pillar

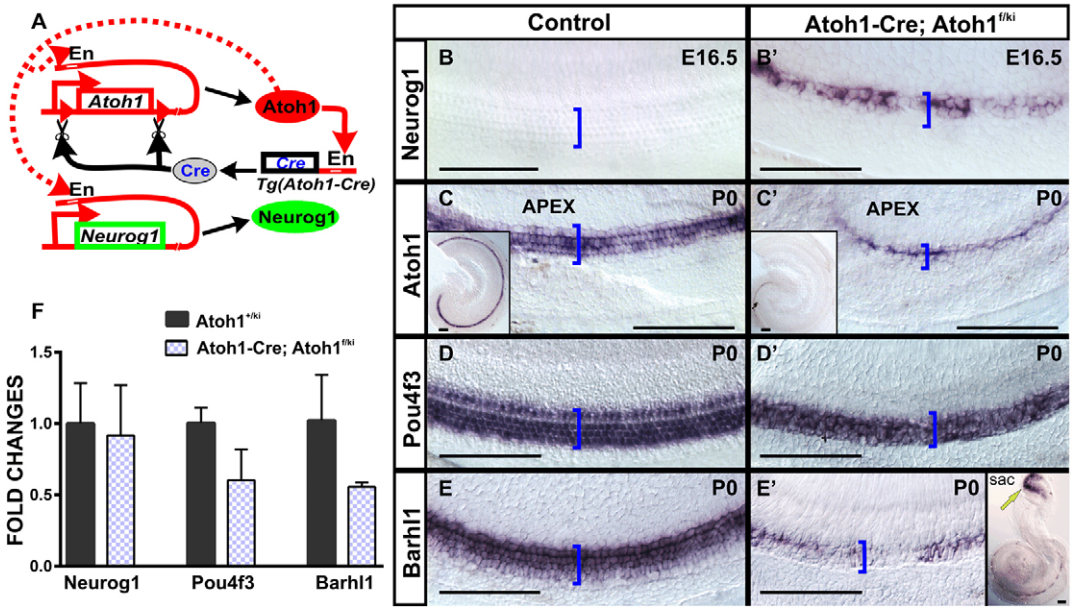

Fig. 1. Our mouse model combines *Atoh1-Cre*, a floxed *Atoh1* allele and an *Atoh1* allele replaced by *Neurog1*. (A) *Atoh1-Cre* uses an *Atoh1* enhancer (En) activated by Atoh1 protein to generate Cre recombinase to excise the floxed *Atoh1* allele. (B-E′) ISH shows misexpression of *Neurog1* in mutant HCs (B′) and its absence in control littermate (B). By contrast, *Atoh1* shows weak expression in one row of cells in the apical tip of the cochlea in *Atoh1-Cre; Atoh1*$^{f/kiNeurog1}$ mice (C′ and inset) compared with broad expression in control littermate (C and inset). *Pou4f3* shows near identical expression in mutant and control littermates (D,D′). By contrast, *Barhl1* is reduced in the cochlea compared with vestibular epithelia in *Atoh1-Cre; Atoh1*$^{f/kiNeurog1}$ mice (E′, yellow arrow in inset) compared with the control littermate (E). Brackets mark the OC. (F) qPCR analysis in P7 cochlea indicates that relative expression of *Neurog1*, *Pou4f3* and *Barhl1* are reduced in *Atoh1-Cre; Atoh1*$^{f/kiNeurog1}$ cochlea compared with *Atoh1*$^{+/kiNeurog1}$ cochlea, but are not statistically significant (P=0.8, 0.07 and 0.2, respectively). (*Atoh1*$^{+/kiNeurog1}$ expression was normalized to 1). Each qPCR data represents the mean of two to three biological and three technical replicates. Error bars represent s.d. Scale bars: 100 µm.

Development (2015) 142, 2810-2821 doi:10.1242/dev.123091

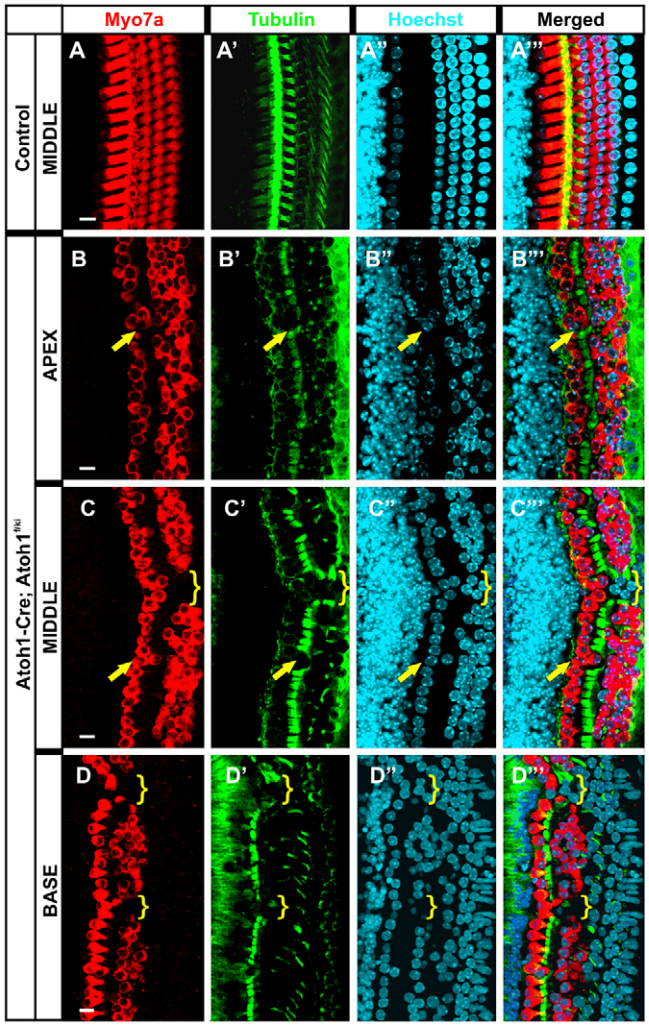

Fig. 2. Misexpression of *Neurog1* results in differentiation of HCs and SCs. Myo7a (HC) and tubulin (SC) immunohistochemistry in P7 *Atoh1-Cre; Atoh1*^{flkiNeurog1} mice shows one row of IHCs and two to three rows of OHCs with near normal SCs (A-D‴). There is loss of the third row of OHCs (D-D‴) and gaps in OHCs (brackets in C-D‴) towards the base of the cochlea. Some additional IHCs are associated with a loss of IP cells (arrows in B-C‴). Scale bars: 10 µm.

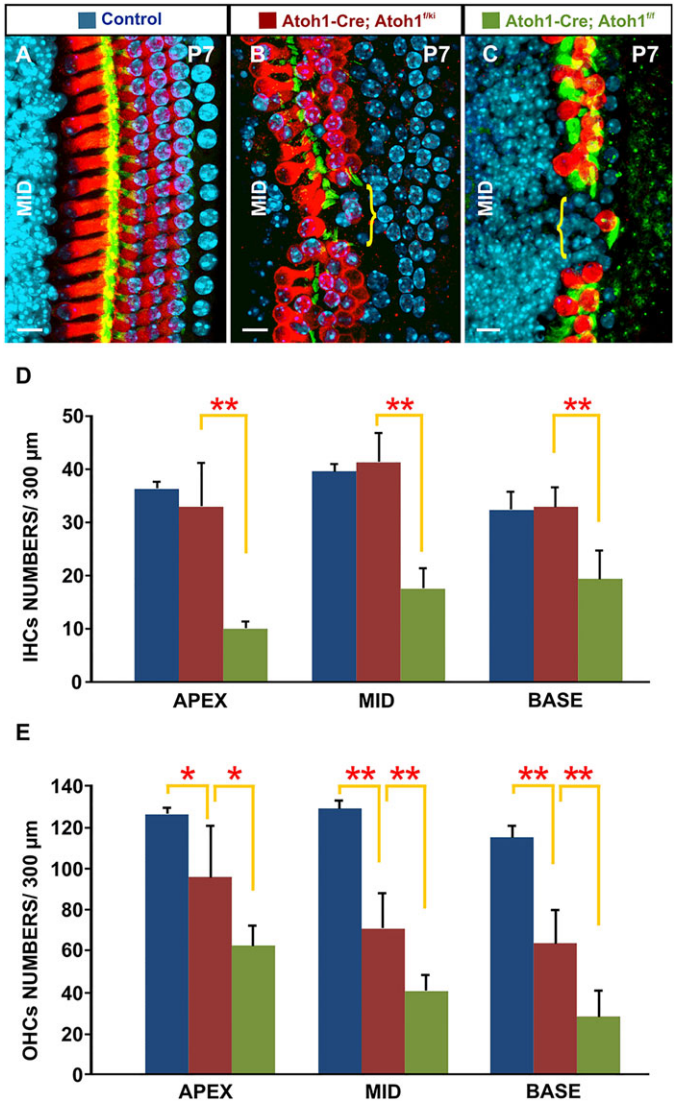

Fig. 3. Misexpression of *Neurog1* rescues IHC formation. (A-C) Myo7a-positive HCs in *Atoh1-Cre; Atoh1*^{flkiNeurog1} cochlea are compared with those in equivalent segments of *Atoh1-Cre; Atoh1*$^{fl/f}$ and control littermates at P7. The *Atoh1-Cre; Atoh1*^{flkiNeurog1} cochlea has more HCs (B), in contrast to a few patchy IHCs and one row of OHCs in the *Atoh1-Cre; Atoh1*$^{fl/f}$ cochlea (C). Brackets highlight gaps in HCs. (D) Quantification of HCs reveals that the numbers of IHCs in *Atoh1-Cre; Atoh1*^{flkiNeurog1} mice (red bar) are significantly higher than those in *Atoh1-Cre; Atoh1*$^{fl/f}$ mice (green bar) but are comparable to those of control littermates (blue bar) in all three areas. (E) However, OHC numbers are reduced in *Atoh1-Cre; Atoh1*^{flkiNeurog1} mice compared with the control (blue bar), but are significantly above those in *Atoh1-Cre; Atoh1*$^{fl/f}$ mice (green bar). Misexpression of *Neurog1* preferentially rescues IHC formation. Each bar represents the mean of six cochleae. Error bars represent s.d. **P*<0.05, ***P*<0.01. Scale bars: 10 µm.

(OP) cells and many Deiters' cells at P7 (Fig. 2). Overall, *Neurog1* misexpression resulted in a considerable increase in HC and SC formation as compared with *Atoh1-Cre; Atoh1*$^{f/f}$ mice, which mostly had one row of OHCs and only a few IHCs at P7 (Fig. 3).

We conclude that *Neurog1* misexpression combined with transient *Atoh1* expression can partially substitute for *Atoh1* to differentiate and maintain HCs, as compared with the massive loss of nearly all HCs in self-terminating mice (Pan et al., 2012a). Diminished long-term viability of HCs correlates with reduced expression of TFs known to be essential for HC viability (*Pou4f3*, *Barhl1*).

More HCs form in *Atoh1-Cre; Atoh1*^{flkiNeurog1} than in *Atoh1-Cre; Atoh1*$^{fl/f}$ mice

We next quantified the Myo7a-positive HCs, identifying IHCs as being medial and OHCs lateral to the tubulin-immunopositive IP/OP cells. We counted all cells in a 300 µm stretch near the apex (10%), near the middle (50%) or near the base of the cochlea (90%) in comparable segments from control, *Atoh1-Cre; Atoh1*$^{f/kiNeurog1}$ and *Atoh1-Cre; Atoh1*$^{f/f}$ littermates (Fig. 3D,E; supplementary material Table S2; n=6). The numbers of IHCs were significantly higher in *Atoh1-Cre; Atoh1*$^{f/kiNeurog1}$ than in *Atoh1-Cre; Atoh1*$^{f/f}$ mice (Fig. 3D; P<0.01). IHC counts between *Atoh1-Cre; Atoh1*$^{f/kiNeurog1}$ mice and control littermates showed no significant difference (Fig. 3D). In summary, replacement of one allele of *Atoh1* by *Neurog1* combined with a self-terminating second *Atoh1* allele rescued most IHCs as compared with the massive loss of IHCs in the *Atoh1-Cre; Atoh1*$^{f/f}$ mouse.

The quantification of OHCs demonstrated that significantly more OHCs form in *Atoh1-Cre; Atoh1*$^{f/kiNeurog1}$ compared with *Atoh1-Cre; Atoh1*$^{f/f}$ mice (Fig. 3E; in the apex, P<0.05; in the

Development (2015) 142, 2810-2821 doi:10.1242/dev.123091

middle and base of the cochlea, $P<0.01$). In contrast to IHCs, OHCs in *Atoh1-Cre; Atoh1*$^{f/kiNeurog1}$ mice were significantly reduced compared with control littermates (Fig. 3E; in the apex, $P<0.05$; in the middle and base of the cochlea, $P<0.01$). Misexpression of *Neurog1* increased survival preferentially of IHCs, with the greatest reduction in the third row of OHCs (Fig. 2C-D‴, Fig. 3B,E). Previous work on self-terminating *Atoh1* conditional null mice (Pan et al., 2012a) and *Atoh1* hypomorphs (Sheykholeslami et al., 2013) showed a differential loss of OHCs, with the third row being most susceptible, whereas tamoxifen-induced *Atoh1-Cre* wiped out all HCs rapidly (Cai et al., 2013; Chonko et al., 2013).

HCs survive longer in *Atoh1-Cre; Atoh1*^{flkiNeurog1} than in *Atoh1-Cre; Atoh1*$^{f/f}$ mice

We next investigated the longevity of these HCs using Myo7a and tubulin immunohistochemistry (Fig. 4). At 9 months, many Myo7a-positive HCs remained in the *Atoh1-Cre; Atoh1*$^{f/kiNeurog1}$ mice. In particular, many IHCs (medial to the tubulin-positive IP cells) survived, but OHCs showed patchy loss (Fig. 4B-B″). This contrasted with severe HC loss in *Atoh1-Cre; Atoh1*$^{f/f}$ mice, where only a few HCs survived up to 9 months (Fig. 4C-C″), essentially being largely lost by 3 weeks (Pan et al., 2012a). In addition to HCs, SCs also persisted longer in *Atoh1-Cre; Atoh1*$^{f/kiNeurog1}$ mice and many more tubulin-positive pillar cells and Deiters' cells were observed compared with *Atoh1-Cre; Atoh1*$^{f/f}$ mice (Fig. 4B′,B″,C′,C″).

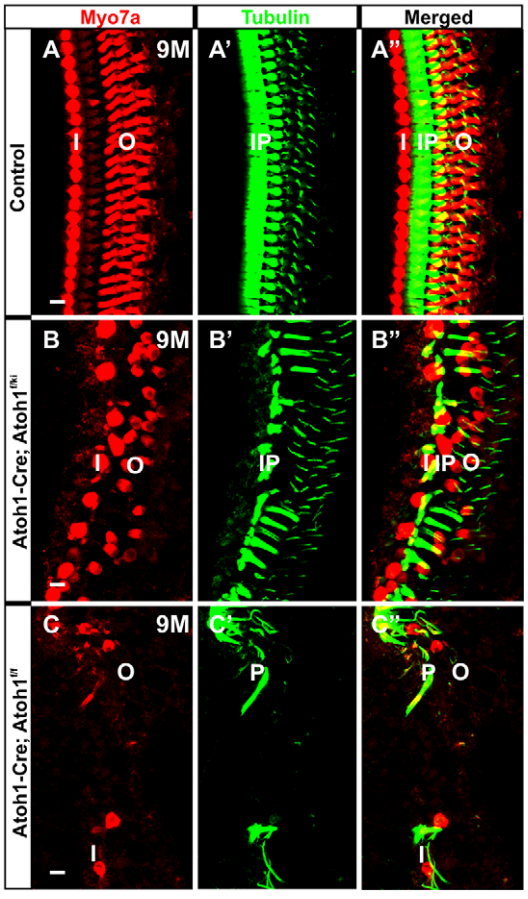

Fig. 4. *Neurog1* misexpression improves longevity of IHCs. Immunohistochemistry of Myo7a and tubulin shows that, compared with the control (A-A″), both IHCs and OHCs and many SCs survive until 9 months in *Atoh1-Cre; Atoh1*^{flkiNeurog1} mice (B-B″). By contrast, only some rare OHCs and SCs survive in the *Atoh1-Cre; Atoh1*$^{f/f}$ littermate (C-C″). IP, inner pillar cell; I, IHC; O, OHC; P, pillar cell (inner/outer). Scale bars: 10 µm.

Atoh1-Cre; Atoh1^{flkiNeurog1} mice are deaf, despite the presence of most HCs

The proper arrangement of cells is essential for the function of the OC to enable sound perception (Cai et al., 2003; Jacobo and Hudspeth, 2014). To assess hearing function in *Neurog1*-misexpressing mice, we measured the auditory brainstem response (ABR) to click stimuli at P30 (Fig. 5). *Atoh1-Cre; Atoh1*$^{f/kiNeurog1}$ mice showed no ABR, in contrast to control littermates (Fig. 5). We concluded that the expression of *Neurog1* facilitates the development and maintenance of many HCs in a non-functional OC. We next investigated possible reasons for this functional defect, focusing first on the stereocilia of HCs.

Replacing *Atoh1* by *Neurog1* results in aberrant stereocilia bundle formation

HC function depends on the normal development of the stereocilia bundles that mediate mechanotransduction (Hudspeth, 2014; Jacobo and Hudspeth, 2014; Sienknecht et al., 2014). Loss, alteration or reduction of *Atoh1* results in abnormal stereocilia bundle formation (Chonko et al., 2013; Pan et al., 2012a), if any bundle forms at all (Pan et al., 2011). *Atoh1* dosage and timing of expression are important for proper stereocilia development and maturation (Jahan et al., 2013). Several mutations that interfere with stereocilia bundle organization and homeostasis are known (Hertzano et al., 2008; Kitajiri et al., 2010; Mogensen et al., 2007; Sekerková et al., 2011) and many of these result not only in aberrant bundle morphology but also in the death of HCs (Kersigo and Fritzsch, 2015; Self et al., 1998; Ueyama et al., 2014). Consistent with a role of *Atoh1* in stereocilia differentiation, forced expression of *Atoh1* can restore hair bundles (Yang et al., 2012).

To extend our findings beyond the obvious increase in HC survival (Figs 2–4) and to better understand the apparent deafness (Fig. 5), we next investigated how replacement of *Atoh1* with *Neurog1* influences stereocilia formation and thus the function of HCs. We examined at least three cochlea of the *Atoh1-Cre; Atoh1*$^{f/kiNeurog1}$ mutant and littermate controls, each at three different stages (P1, P7 and P22), by scanning electron microscopy (SEM) (Figs 6 and 7). We found that the onset of stereocilia bundle differentiation in *Neurog1*-misexpressing mice was delayed (Fig. 6A-B″). The bundles were immature, with the formation of

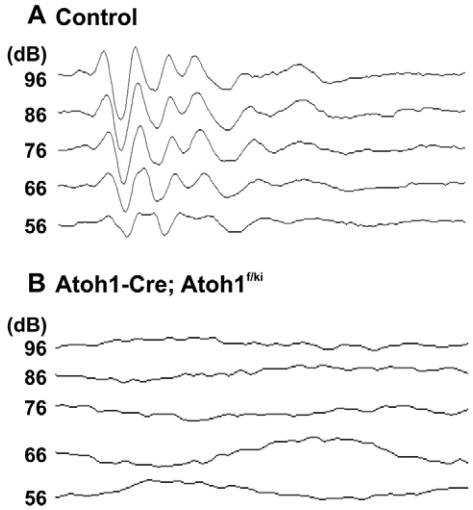

Fig. 5. *Atoh1-Cre; Atoh1*^{flkiNeurog1} mice show no ABR response. P30 *Atoh1-Cre; Atoh1*^{flkiNeurog1} mice show no click response in ABR (B), in contrast to the control (A), indicating severe deafness over the intensity range tested.

Development (2015) 142, 2810-2821 doi:10.1242/dev.123091

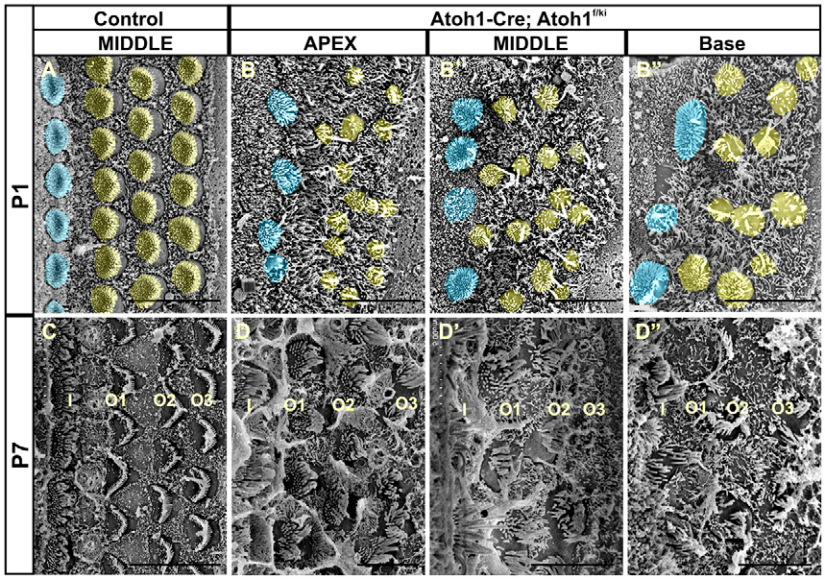

Fig. 6. Delayed onset of maturation of stereocilia bundles in *Atoh1-Cre; Atoh1$^{f/kiNeurog1}$* mice. SEM shows that stereocilia bundles remain immature with central kinocilia at P1 in *Atoh1-Cre; Atoh1$^{f/kiNeurog1}$* mice (B-B″) and there is no staircase pattern, in contrast to control littermates (A). This delay is most evident in OHCs (B-B″). In P7 *Atoh1-Cre; Atoh1$^{f/kiNeurog1}$* cochlea, the stereocilia bundles in the apical HCs form a near normal staircase pattern (D,D′), as compared with the control (C), whereas the third row of basal OHCs shows aberration (D″). A portion of HCs are color coded (A-B″) for better visibility: IHCs in cyan and OHCs in yellow. I, IHC; O1-O3, 1-3 rows of OHCs. Scale bars: 5 µm in A-B″,D-D″; 10 µm in C.

microvilli that were all similar in length surrounding a central kinocilium at P1 (Fig. 6B-B″). Control littermates already displayed the staircase pattern of progressively increasing length of stereocilia modiolar to an acentric kinocilium (Fig. 6A). This stunted stereocilia growth was more obvious in OHCs than IHCs, especially in the second and third rows of OHCs of *Atoh1-Cre; Atoh1$^{f/kiNeurog1}$* mice. In *Atoh1-Cre; Atoh1$^{f/kiNeurog1}$* mice at P7, the bundles formed a nearly normal staircase pattern in the apex of the cochlea, whereas the basal HCs displayed aberrations such as fusion or loss of stereocilia, predominantly in the third row of OHCs (Fig. 6C-D″).

SEM revealed progressive deformations of the stereocilia bundles in *Atoh1-Cre; Atoh1$^{f/kiNeurog1}$* mice (Fig. 7). Some HCs in the *Neurog1*-misexpressing mice had stereocilia bundles that lacked the staircase organization, and some stereocilia were fused with each other or showed stunted growth (cyan arrows in Fig. 7). SEM also revealed that the thickness of the stereocilia of some IHCs in *Atoh1-Cre; Atoh1$^{f/kiNeurog1}$* mice was altered to resemble OHCs, indicating partial cell fate switching of some IHCs to OHCs (red arrows in Fig. 7). Beyond the fusion and ectopic stereocilia formation, SEM in the *Neurog1*-misexpressing mice also revealed disruption of the boundaries between adjacent HCs (Fig. 7). Some HCs touched each other without intervening SCs in *Atoh1-Cre; Atoh1$^{f/kiNeurog1}$* mice (green arrows in Fig. 7). At P7 and P22, we found ectopic stereocilia bundles protruding from the apical surfaces of the IP cells (yellow arrows, Fig. 7). This altered pattern of HCs and SCs indicated disruptions of cell-cell interactions. We therefore further analyzed the molecular basis of OC pattern formation (Fritzsch et al., 2014b; Groves and Fekete, 2012), focusing on genes known to affect OC development.

We previously demonstrated conversion of OHCs into IHCs in *Neurod1* conditional deletion mice (Jahan et al., 2010). Absence of *Neurod1* resulted in premature and altered *Atoh1* and *Fgf8* expression and transformation of thin OHC stereocilia into thick IHC stereocilia (Jahan et al., 2010, 2013). Essentially, *Atoh1* and *Fgf8* expression failed to be suppressed by *Neurod1* in *Neurod1* conditional deletion mice (Jahan et al., 2010). We investigated the expression of *Neurod1* and *Fgf8* in the *Atoh1-Cre; Atoh1$^{f/kiNeurog1}$* mice, as they showed the opposite effect, i.e. conversion of stereocilia of IHCs to OHCs. Misexpression of *Neurog1* resulted in stronger and earlier expression of *Neurod1* in E16.5 *Atoh1-Cre; Atoh1$^{f/kiNeurog1}$* cochlea as compared with control littermates (Fig. 8A-B″). *Fgf8* expression was patchy and much reduced in some IHCs of the E16.5 *Atoh1-Cre; Atoh1$^{f/kiNeurog1}$* mice (Fig. 8D′; supplementary material Fig. S1B′). The alteration of HC stereocilia diameter in *Atoh1-Cre; Atoh1$^{f/kiNeurog1}$* mice might relate to the locally altered level of *Atoh1*/*Neurog1* signaling that distorted the specificity of HC types. How alteration of *Atoh1* signal level mechanistically regulates the thickness of the stereocilia bundles, possibly through modulation of whirlin (Mogensen et al., 2007), requires further work.

Among microRNAs (miRNAs), miR-96 was specifically reported as being required for the proper maturation and organization of the stereocilia bundle (Kuhn et al., 2011; Lewis et al., 2009). Single base mutation in the *MIR96* gene results in non-syndromic, progressive hearing loss in humans (Kuhn et al., 2011; Lewis et al., 2009). miR-96 is expressed in the sensory epithelia of the mouse cochlea (Weston et al., 2011). We previously reported very limited miR-96 expression only in the apex of *Atoh1$^{kiNeurog1/kiNeurog1}$* cochlea (Jahan et al., 2012) or its near absence in conditional *Atoh1* null mice (Pan et al., 2011). Both mutants showed no HC differentiation beyond precursors cells. In the *Atoh1-Cre; Atoh1$^{f/kiNeurog1}$* mice, miR-96 expression was almost normal, except for the basal hook region where it showed some gaps (Fig. 8E-F′). How possible alterations in some miRNAs tie into stereocilia development through the repression of relevant genes remains speculative.

Neurog1 misexpression alters OC patterning and SC differentiation

Given the formation of stereocilia bundles on IP cells (Fig. 7), we next investigated the distribution of an IP cell-specific marker, *p75* (*Ngfr*) (von Bartheld et al., 1991). ISH of *p75* confirmed its selective expression in IP cells in P0 control mice (Fig. 9A). In P0 *Atoh1-Cre; Atoh1$^{f/kiNeurog1}$* mice, *p75* expression was patchy near the base (Fig. 9B′,B″) but continuous in the apical half (Fig. 9B) of the cochlea. Consistent with stereocilia bundles on IP cells (Fig. 7A-C, E), immunohistochemistry for the HC-specific Myo7a subsequent to *p75* ISH showed that the gaps in the *p75*-positive IP cells were filled with Myo7a-positive HCs (Fig. 9B″). We also performed dual immunohistochemistry using p75 and Myo7a antibodies with different fluorophore labeling of the secondary antibodies. This also showed that the gaps in p75-immunopositive IP cells were filled

Development (2015) 142, 2810-2821 doi:10.1242/dev.123091

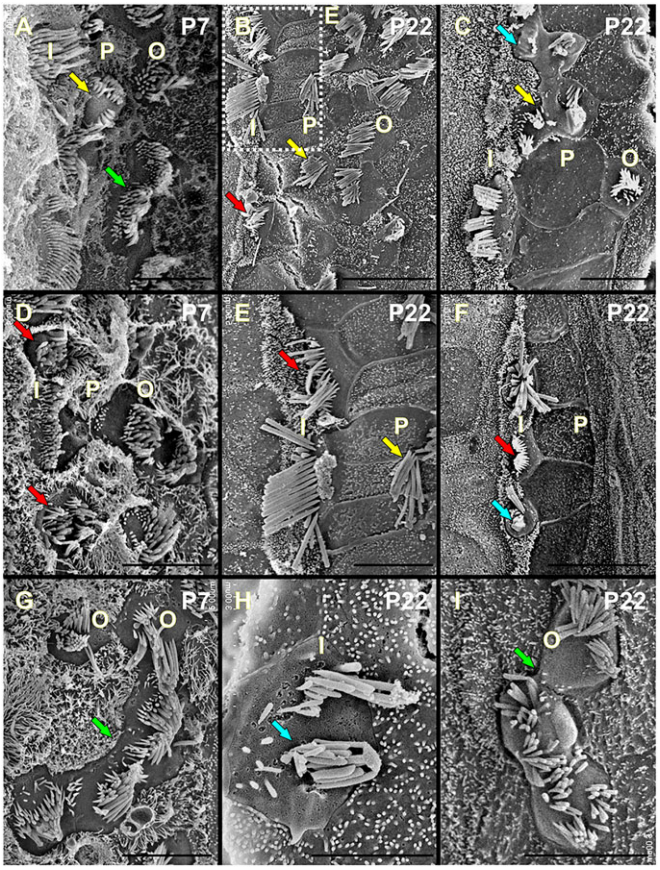

Fig. 7. *Neurog1* misexpression results in alteration in stereocilia bundle thickness, cell fate changes and disruption of cell-cell interactions. Although *Neurog1* misexpression shows near normal HC formation (Figs 2-4), HC type and topology-specific stereocilia bundle formation at P7 (A,D,G) and P22 (B,C,E,F,H,I) are disorganized. Ectopic HCs form in the position of IP cells, as revealed by formation of stereocilia bundles from their apical surfaces (yellow arrows in A-C,E). In addition, *Neurog1* misexpression results in transdifferentiation of IHCs into OHCs, as demonstrated by the appearance of thin stereocilia of OHCs in the position of IHCs (red arrows in B,D-F). Some OHCs are in broad continuity with each other (green arrows in A,G,I) and some stereocilia bundles are fused or stunted in growth (cyan arrows in C,F,H). *Neurog1* misexpression results in irregular stereocilia formation in most HCs, that gradually deteriorate with age. I, IHC; O, OHC; P, pillar cell. Scale bars: 5 µm in A,C-E,G,H; 10 µm in B,F; 3 µm in I.

with Myo7a-positive putative HCs (Fig. 9C-D″). Combined with stereocilia formation in the apical surfaces of the IP cells of *Atoh1-Cre; Atoh1*$^{f/kiNeurog1}$ mice, our data suggested that expression of *Neurog1* transformed some IP cells into a hybrid of IP and HC.

To further assess this possibility, we quantified the tubulin-immunopositive IP cells in P7 *Atoh1-Cre; Atoh1*$^{f/kiNeurog1}$ mice (Fig. 9E). There was a reduction of tubulin-positive IP cells in the *Neurog1*-misexpressing mice relative to control littermates in the apex (P<0.05) and middle (P<0.01) turn of the cochlea. Despite this presumed transformation, overall IP cell formation was increased in *Atoh1-Cre; Atoh1*$^{f/kiNeurog1}$ relative to *Atoh1-Cre; Atoh1*$^{f/f}$ mice (P<0.01). Although p75 is an excellent marker for IP cells, differentiation of IP cells remains normal in *p75* null mice and its function in IP cells remains obscure (Tan et al., 2010).

Pillar cell formation is abnormal in *Fgf8* null mice (Jacques et al., 2007; Mueller et al., 2002). As previously reported (Jacques et al., 2007; Pirvola et al., 2000), *Fgf8* is expressed in all IHCs. In the *Atoh1-Cre; Atoh1*$^{f/kiNeurog1}$ mice, downregulation of *Fgf8* expression might affect the strength of diffusible signal from IHCs to nearby SCs (Groves and Fekete, 2012). Given the defects in IP cells, we next performed double ISH for *Fgf8* and *p75* and revealed that the reduction of *Fgf8* expression correlated with that of *p75* in *Atoh1-Cre; Atoh1*$^{f/kiNeurog1}$ mice (supplementary material Fig. S1A-C′). Previous work also demonstrated that *Atoh1* is transiently expressed in IP cells (Driver et al., 2013; Matei et al., 2005). Signals that prevent IP cells from differentiating as HCs might be disrupted in the *Atoh1-Cre; Atoh1*$^{f/kiNeurog1}$ mice, resulting in partial transdifferentiation of some IP cells into HCs (Fig. 7).

We also investigated the *Fgf10* and *Bmp4* expression that flanks the medial and lateral borders of the OC, respectively (supplementary material Fig. S1D,D′). In P0 *Atoh1-Cre; Atoh1*$^{f/kiNeurog1}$ mice, *Fgf10* was drastically reduced and *Bmp4* showed expanded expression toward OC, with gaps where OC cells were replaced by simple epithelium (supplementary material Fig. S1D,D′).

To obtain further molecular insight into SC differentiation, we studied *Prox1* expression by ISH in the *Neurog1*-misexpressing mice (Fritzsch et al., 2010a). *Prox1* was expressed in almost all SCs, except for some reduction in the IP cells in P0 *Atoh1-Cre; Atoh1*$^{f/kiNeurog1}$ mice (Fig. 10A-B″). These data suggested that several reliable markers of SC differentiation were altered, lost or even replaced by HC markers, indicating that expression of *Neurog1* in HCs affected other cells of the OC.

Neurog1 expression alters Notch ligand and Notch effector gene expression

Atoh1 expression in HCs regulates the expression of genes in the Delta/Notch signaling pathway that are necessary for the development of the surrounding SCs and maintains the proper patterning of the OC (Kobayashi and Kageyama, 2014; Sprinzak et al., 2011; Yamamoto et al., 2014). Lack of the Notch ligand *Jag1* results in extra rows of IHCs and the loss of OHCs (Brooker et al., 2006; Kiernan et al., 2006). The Hes/Hey factors, which are downstream target genes of Notch, play important roles in the proper specification of SCs by negatively regulating pro-neuronal bHLH TFs (Doetzlhofer et al., 2009; Zine and de Ribaupierre, 2002). Given the lack of proper patterning of HCs/SCs in the OC, we investigated the expression of *Jag1* and *Hes5* by ISH in *Atoh1-Cre; Atoh1*$^{f/kiNeurog1}$ mice (Fig. 10). In the P0 control mice, *Jag1* was widely expressed in the greater epithelial ridge (GER) and in SCs, particularly in the IP cells (Fig. 10C,C′). In *Atoh1-Cre; Atoh1*$^{f/kiNeurog1}$ mice, the expression of *Jag1* was slightly reduced in both the GER and SCs, with some patchy loss toward the cochlear base (Fig. 10D,D′).

At E14.5, *Hes5* was found in the mid-base of control cochlea (supplementary material Fig. S2A). E14.5 *Atoh1-Cre; Atoh1*$^{f/kiNeurog1}$ mice had delayed *Hes5* expression (supplementary material Fig. S2D); *Hes5* was upregulated at later stages (supplementary material Fig. S2E,F) and showed patchy expression in the GER and in SCs (Fig. 10E-F″; supplementary material Fig. S2E,F). We combined *Hes5* ISH with Myo7a immunohistochemistry to detect whether the downregulation of *Hes5* was associated with HC differentiation in the *Neurog1*-misexpressing mice (supplementary material Fig. S2G-H″), as previously reported after *Hes5* loss (Zine and de Ribaupierre, 2002). Myo7a-positive HCs showed no correlation with the patchy loss of *Hes5* expression in this mutant (supplementary material Fig. S2G-H″).

Alteration of *Jag1* and *Hes5* expression in *Atoh1-Cre; Atoh1*$^{f/kiNeurog1}$ mice indicated the potential effects of *Neurog1* on the expression of these genes, and thus on Delta/Notch signaling. This altered HC-SC communication might disrupt OC patterning

Development (2015) 142, 2810-2821 doi:10.1242/dev.123091

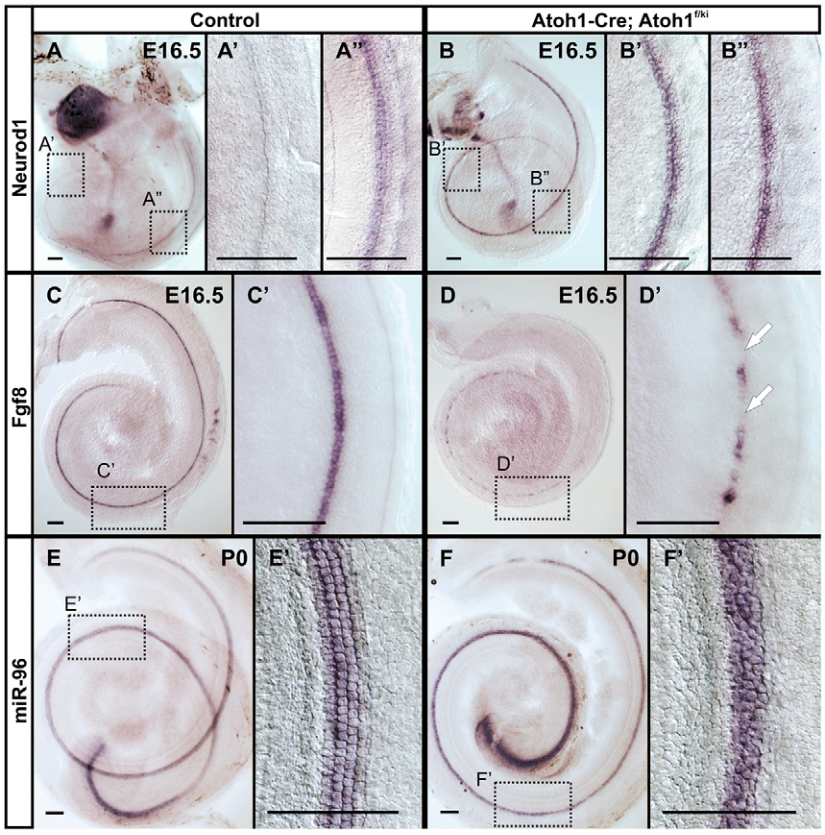

Fig. 8. *Neurog1* misexpression induces premature *Neurod1* upregulation and suppresses *Fgf8* but not miR-96 expression. ISH shows that expression of *Neurod1* expands both longitudinally and radially in the HCs of *Atoh1-Cre; Atoh1*$^{f/kiNeurog1}$ cochlea as compared with the control littermate, in which expression is limited to IHCs (A-B″). *Fgf8* expression displays patchy downregulation (arrows) in the E16.5 *Atoh1-Cre; Atoh1*$^{f/kiNeurog1}$ cochlea (C-D′). This suppression of *Fgf8* might in part be regulated by *Neurod1* overexpression in *Atoh1-Cre; Atoh1*$^{f/kiNeurog1}$ mice (B,B′,D,D′), as previously suggested (Jahan et al., 2010). miR-96, an essential miRNA for stereocilia differentiation, shows no expression changes in HCs (E-F′). Scale bars: 100 µm.

(Fig. 7), but did not result in an overproduction of HCs (supplementary material Fig. S2H-H″), unlike in Hes/Hey mutants (Benito-Gonzalez and Doetzlhofer, 2014; Zine et al., 2001). How changes in intracellular HC gene expression through replacement of *Atoh1* by *Neurog1* alter intercellular signaling and disrupt the mosaic of the OC remains unclear.

In conclusion, near normal numbers of HCs can be generated by combining transient *Atoh1* expression with *Neurog1* misexpression, but these HCs have variably defective stereocilia bundles and the OC is disorganized. Despite long-term viable HCs, the abnormal OC organization causes deafness. OC disorganization may be a consequence of changes in *Fgf8* expression, which might lead to the formation of secondary signaling centers comparable to the midbrain hindbrain boundary (Fritzsch et al., 2014a; Lee et al., 1997), or may also be due to altered cellular interactions (Groves and Fekete, 2012).

DISCUSSION

A fundamental aim in the study of neurosensory development, and in the context of regeneration in particular, is understanding the molecular basis for the generation of topologically distinct cell fates from uniform progenitor populations (Fritzsch et al., 2014a; Imayoshi and Kageyama, 2014; Reiprich and Wegner, 2015). Precise spatial and temporal control of gene expression by different combinations of TFs establish the molecular code that determines cell fate (Guillemot, 2007). Molecular dissection of this complexity requires models of limited cellular diversity in a stereotyped arrangement to evaluate minute deviations from normal; for example, in the ommatidia of flies (Johnston and Desplan, 2014). The OC of the mammalian inner ear is another excellent model organ with stereotyped cellular patterning that allows the exploration of molecularly induced deviations of developmental processes mediated by intracellular and extracellular patterning processes (Fritzsch et al., 2014b; Groves and Fekete, 2012). Our data suggest a profound effect of intracellular signals via cell-cell interactions and alterations in diffusible factors on the cellular and organ patterning process.

Neurog1 cooperates with transient *Atoh1* expression to develop and maintain HCs

One approach to probing the signal specificity of a given TF in developing gene regulation networks is to replace them by closely related TFs (Guillemot, 2007). Replacing *Atoh7* with *Neurod1* leads to normal differentiation of RGCs, whereas replacing *Neurod1* by *Atoh7* alters the cell fate of amacrine and photoreceptor cells into RGCs (Mao et al., 2013, 2008), indicating context dependency of gene actions. We knocked *Neurog1* into the *Atoh1* locus to test whether a bHLH TF that is exclusively associated with proliferative precursors in the ear and brain (Imayoshi and Kageyama, 2014; Ma et al., 2000) can function in differentiation to maintain or alter HC precursor differentiation. We previously showed that *Atoh1*$^{kiNeurog1/kiNeurog1}$ can effectively drive *Neurod1* in HC precursors (Jahan et al., 2012) but can neither initiate normal HC development nor maintain the viability of HC precursors. We also showed that self-terminating *Atoh1* results in very limited viability of HCs, with incomplete stereocilia differentiation (Pan et al., 2012a). Our quantitative assessment of HC formation in *Atoh1-Cre; Atoh1*$^{f/kiNeurog1}$ mice in this study indicates that *Neurog1* misexpression partially rescues HCs and maintains HCs for a longer period, as compared with self-terminating *Atoh1* conditional null mice (Pan et al., 2012a). *Neurog1* cannot maintain the basal third row of OHCs that depends on Fgf20 released from SCs (Huh et al., 2012), a factor that might be affected in our mice due to alteration in SC development.

Our data suggest that HC precursors behave like RGCs (Mao et al., 2008) and show limited flexibility to respond to the distantly

Development (2015) 142, 2810-2821 doi:10.1242/dev.123091

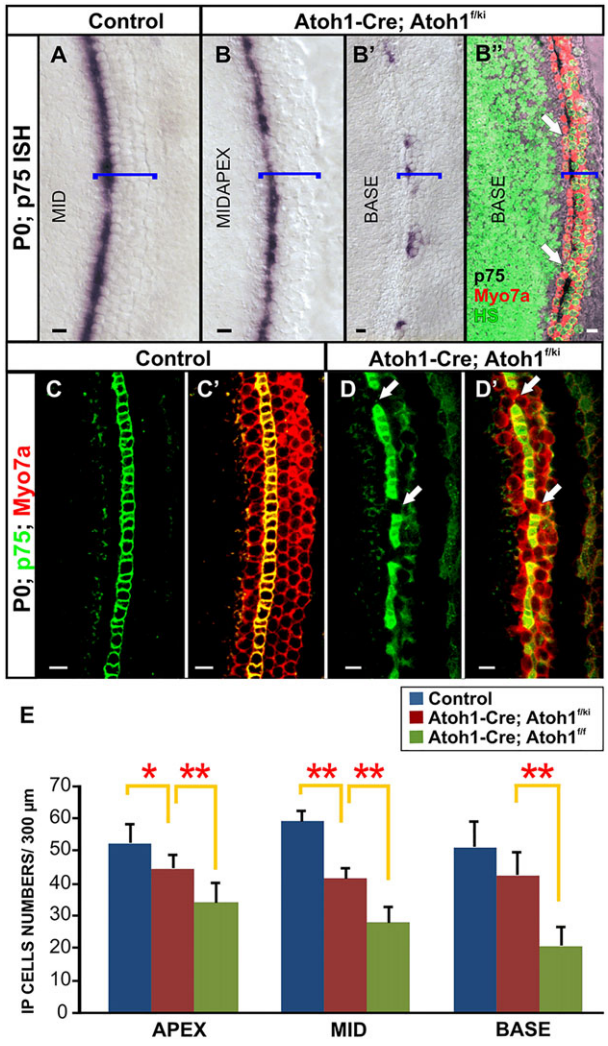

Fig. 9. Myo7a-positive 'HCs' fill gaps in *p75*-negative IP cells in *Atoh1-Cre; Atoh1*$^{f/kiNeurog1}$ mice. ISH of *p75* shows continuous expression in IP cells in the apical half (mid), comparable to the control littermates, but the presence of gaps in the base (A-B″). Bracket specifies the OC. Combining Myo7a immunohistochemistry with the *p75* ISH-positive cochlea shows that some Myo7a-positive 'HCs' form in the gaps between *p75*-positive IP cells (arrows in B″), as further confirmed (arrows in D,D′) by double immunohistochemistry of p75 and Myo7a (C-D′). Quantification of IP cells (E) demonstrates decreased numbers in *Atoh1-Cre; Atoh1*$^{f/kiNeurog1}$ mice compared with control littermates, but significantly increased numbers compared with those in *Atoh1-Cre; Atoh1*$^{f/f}$ littermates. **P*<0.05, ***P*<0.01. Each bar represents the mean of six cochleae. Error bars represent s.d. Scale bars: 10 µm.

related bHLH TF *Neurog1* beyond enhanced HC differentiation relative to that of transient *Atoh1* expression. This differs from spiral ganglion neurons, which differentiate readily as HCs if suppression of *Atoh1* is removed by eliminating *Neurod1* (Jahan et al., 2010). *Atoh1* is required for an uncharacterized initial step of HC differentiation that neither *Neurog1* nor *Neurod1* can replace, and thus no HCs differentiate in homozygotic *Atoh1*$^{kiNeurog1/kiNeurog1}$ mice (Jahan et al., 2012). The fly *atonal* gene can replace *Atoh1* (Wang et al., 2002) and HCs can partially differentiate with the reduced (Sheykholeslami et al., 2013) or transient (Pan et al., 2012a) expression of *Atoh1*, or even in the absence of *Atoh1* in chimeric mice (Du et al., 2007). Elucidating the molecular basis of this critical step of downstream gene activation (Cai et al., 2015; Pan et al., 2012b), in which *Atoh1* expression cannot be substituted by *Neurog1*, could help to transform stem cells more effectively into HCs (Ronaghi et al., 2014; Zine et al., 2014).

Atoh1 cooperates with unknown factors to fully express *Pou4f3* (Ahmed et al., 2012), which, in turn, cooperates with *Atoh1* to maintain HCs (Chen et al., 2015; Hertzano et al., 2004; Masuda et al., 2012; Xiang et al., 2003). In contrast to *Pou4f3*, *Barhl1* expression depends exclusively on *Atoh1* (Chellappa et al., 2008). *Barhl1* is required for HC survival even in the presence of *Atoh1* and *Pou4f3* (Li et al., 2002). *Atoh1-Cre; Atoh1*$^{f/kiNeurog1}$ mice have near normal expression of *Pou4f3*, but show a delay and progressive reduction of *Barhl1* (Fig. 1). We suggest that *Neurog1* might activate a second pathway for near normal *Pou4f3* expression (Ahmed et al., 2012; Masuda et al., 2012), but fails to fully activate *Barhl1* needed for HC maintenance (Fig. 11). Our mouse model will prove useful in testing the ability of putative regulators of downstream genes to enhance HC viability through the regulation of *Pou4f3* and *Barhl1* expression.

Replacement of *Atoh1* by *Neurog1* alters stereocilia differentiation

Closer investigation of the cochlea of *Neurog1*-misexpressing mice revealed various irregularities in stereocilia bundles and their distribution in the OC (Figs 6 and 7): the irregular length of individual stereocilia within the bundles; the uncoupling of stereocilia diameter from HC type; the appearance of ectopic stereocilia bundles on IP cells; and stereocilia bundles being abnormally fused with each other.

Stereocilia are necessary for hearing (Müller and Barr-Gillespie, 2015). Despite the rescue of overall HC formation, *Atoh1-Cre; Atoh1*$^{f/kiNeurog1}$ mice show no ABR and are deaf (Fig. 5). Whether this is due to some defect in the HCs or to the disorganization of the OC requires future single-cell recordings on isolated HCs. We presume that the irregularities in stereocilia bundles, which are essential for mechanoelectric transduction (Hudspeth, 2014), preclude the normal function of many HCs. Loss of *Pou4f3*, but not of *Barhl1*, causes stereocilia bundle aberrations (Chellappa et al., 2008; Hertzano et al., 2004). A reduced level of *Pou4f3* transcripts at or after P7 might contribute to the bundle aberration that develops mostly in late postnatal stages in *Neurog1*-misexpressing mice (Fig. 7).

Actin is a major protein component of stereocilia (Müller and Barr-Gillespie, 2015) and stereocilia homeostasis is essential for HC function and viability (Kersigo and Fritzsch, 2015; Self et al., 1999; Ueyama et al., 2014). Dysregulation of actin bundling has been associated with HC dysfunction and loss (Mogensen et al., 2007; Perrin et al., 2010; Rzadzinska et al., 2009; Taylor et al., 2015). Various myosins, actins and a rich variety of actin-bundling proteins are regulated downstream of Atoh1 to transform microvilli into stereocilia during development (Kitajiri et al., 2010; Schwander et al., 2010). Loss of miRNAs is also associated with derailed stereocilia development (Weston et al., 2011). *Neurog1* misexpression results in near normal miR-96 expression, but other miRNAs could be altered that also affect stereocilia formation. Once causality between Atoh1 and downstream signals associated with various bundle aberrations is clearer, our mouse model could help to eliminate spurious relationships as it has partially uncoupled stereocilia differentiation from HC topology.

Replacement of *Atoh1* by *Neurog1* alters the patterning of the OC

The OC is highly stereotyped in organization, with two distinctly patterned compartments separated by a single row of adjacent IP cells, which express *Atoh1* (Driver et al., 2013; Fritzsch et al., 2014b; Matei et al., 2005) without differentiating into HCs.

Development (2015) 142, 2810-2821 doi:10.1242/dev.123091

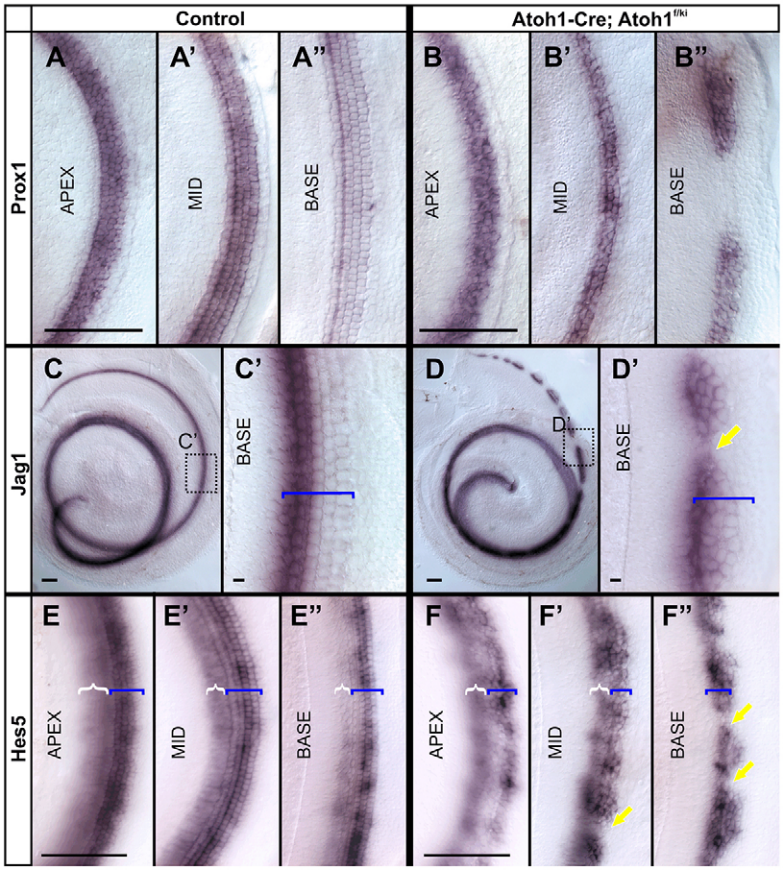

Fig. 10. *Neurog1* misexpression in HCs alters SC marker expression pattern. (A-B″) ISH reveals near normal expression of *Prox1* in SCs, except for some patchy loss in the base of *Atoh1-Cre; Atoh1*^{flkiNeurog1} mice. (C-D′) *Jag1* expression shows patchy loss (arrow in D′) in *Atoh1-Cre; Atoh1*^{flkiNeurog1} mice. (E-F″) *Neurog1* misexpression results in differential loss of *Hes5* expression (arrows in F′,F″). Curved brackets demarcate expression in the GER and square brackets demarcate expression in the OC. Scale bars: 100 µm except 10 µm in C′ and D′.

Expression of multiple Hes/Hey factors (Benito-Gonzalez and Doetzlhofer, 2014; Doetzlhofer et al., 2009; Petrovic et al., 2015) may block these cells from HC development. Notch inhibition (and thus reduced expression of Hes/Hey) may lead to HC differentiation of IP cells (Mizutari et al., 2013). *Neurog1* misexpression affects IP cells in multiple ways, including the formation of HC-like stereocilia bundles and replacement by the HC marker Myo7a in *p75*-positive IP cells. These instabilities in IP cells might relate to the alteration in Notch signaling, as observed (Figs 9 and 10).

In addition, the disruption of OC patterning is in part due to alterations in the Delta/Notch signaling pathway. For example, expression of *Jag1* and of the downstream target gene *Hes5* are altered. Previous work on *Jag1* loss showed a reduction in the total number of HCs (Kiernan et al., 2006). *Neurog1* misexpression results in discontinuity of *Jag1* and delayed upregulation and differential downregulation of *Hes5* in the cochlea. These expression changes vary radially and longitudinally, providing additional modulations of the variable signals of diffusible factors such as Fgf8, Fgf10 and Bmp4. Combined with altered SC response properties through changes in *p75* and *Prox1*, these local changes might relate to the random OC patterning defects.

In summary, we demonstrate that misexpression of *Neurog1* provides partial functional replacement of *Atoh1* in the developing HC and improves HC maintenance. *Neurog1* misexpression changes the signaling pattern of diffusible factors originating from HCs, as well as cell-cell interactions via Delta/Notch; both alterations contribute to the disorganization of the OC. Previous reports on the deletion of different combinations of *Hes1*, *Hes5* or *Hey2* show changes in sensory patterning in support of the lateral inhibition model, but mutants mostly maintain the HC and SC mosaic formation (Doetzlhofer et al., 2009; Zine et al., 2001). Changes of proneural bHLH genes in HCs alters the overall

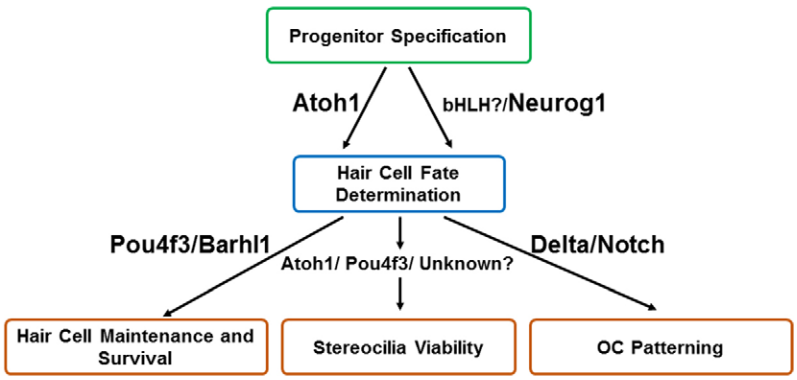

Fig. 11. Role of *Atoh1* and *Neurog1* in HC fate determination. Summary flowchart indicating that *Atoh1* is essential for HC fate determination, in part mediated by an unknown bHLH gene (Ahmed et al., 2012). *Neurog1* may in part mimic this unknown bHLH gene to cooperate with *Atoh1* and maintain the expression of some target genes. However, *Neurog1* cannot fully regulate downstream HC genes associated with stereocilia maturation and OC patterning, leading to disorganization of the OC in the absence of *Atoh1*.

Development (2015) 142, 2810-2821 doi:10.1242/dev.123091

patterning of the OC, presumably by altering intercellular interactions via diffusible factors (Fgf8) and cell-cell interactions.

Understanding the causalities of these alterations and translating such understanding into regeneration (Zine et al., 2014) could help to restore hearing in deaf patients, with deafness now constituting the fastest growing ailment of the elderly worldwide (Kersigo and Fritzsch, 2015; Müller and Barr-Gillespie, 2015). Beyond the addition or deletion of entire rows of HCs obtained with previous mutations (Doetzlhofer et al., 2009; Zine et al., 2001), we provide here a new model of a dysfunctional OC that can help in OC restoration endeavors. Converting, through additional manipulation, the dysfunctional OC of our new mouse model into a functional OC that is able to restore hearing could provide proof of principle for fledgling attempts that aim to transform a partially defunct elderly OC into a fully functional OC.

Note added in proof

The pattern of the organ of Corti was recently summarized by Jahan et al. (2015).

MATERIALS AND METHODS

Ethics guidelines

All animal procedures were carried out according to the recommendations and guidelines of the University of Iowa Institutional Animal Care and Use Committee (IACUC) under approved protocol ACURF #1309175.

Combining *Neurog1* knock-in (*Atoh1*^{kiNeurog1}) with self-terminating *Atoh1* mice (*Atoh1-Cre; Atoh1*$^{f/kiNeurog1}$)

Construction of the *Neurog1* knock-in plasmid and generation of the *Atoh1*^{kiNeurog1} mouse model were described previously (Jahan et al., 2012). To generate the *Atoh1-Cre; Atoh1*$^{f/kiNeurog1}$ line, we bred heterozygous *Neurog1* knock-in mice (*Atoh1*$^{+/kiNeurog1}$) (Jahan et al., 2012) with mice carrying the *Atoh1-Cre* transgene and one *Atoh1* floxed allele (*Atoh1-Cre; Atoh1*$^{f/+}$) as described previously (Pan et al., 2012a).

Genotyping

Mice were genotyped using tail DNA for standard PCR amplification as described previously (Jahan et al., 2012; Pan et al., 2012a). For further details, see the supplementary Materials and Methods.

In situ hybridization

ISH was performed as previously described (Jahan et al., 2012) using RNA probes labeled with digoxigenin. A detailed description is provided in the supplementary Materials and Methods.

RT-qPCR

For quantitative reverse transcription PCR (RT-qPCR), we used cochlea from P7 *Atoh1-Cre; Atoh1*$^{f/kiNeurog1}$ mice and their heterozygous *Atoh1*$^{+/kiNeurog1}$ littermates as control. After sedation with 2,2,2 tribromoethanol, the mice were hemisected and the cochleae were dissected out within 2-3 min in RNase-free conditions and stored in RNAlater (Ambion) at −80°C. Total RNA extraction was performed using the Direct-zol RNA Mini-Prep Kit (Zymo Research) and RNA concentration and 260/280 ratio were obtained with a Nanodrop spectrophotometer. On-column DNase I treatment was performed according to the Direct-zol Kit protocol. 1 µg total RNA was reverse transcribed and cDNA was synthesized with Anchored-oligo $(dT)_{18}$ primer using the Transcriptor First Strand cDNA Synthesis Kit (Roche). For qPCR, the primers and probes were designed using the Roche Universal ProbeLibrary Assay Design Center and primers were obtained from Integrated DNA Technologies. Primer sequences and priming conditions are listed in supplementary material Table S3. qPCR was performed in a 96-well plate using Roche LightCycler 480 Probes Master Mix and a Roche Light Cycler 480 real-time PCR machine. For all target genes, qPCR was performed for at least three to four biological replicates and three technical replicates including no-template controls for each sample following MIQE guidelines (Bustin et al., 2009). qPCR data were analyzed in Microsoft Excel and $\Delta\Delta C_T$ was calculated to determine the relative expression in *Atoh1-Cre; Atoh1*$^{f/kiNeurog1}$ cochlea compared with control normalized to *Actb* reference transcript. Statistical analysis was performed with Student's *t*-test in GraphPad Prism 6 software.

Immunohistochemistry and cell counts

Immunohistochemistry was performed as described previously (Jahan et al., 2012). IHCs, OHCs and IP cells were counted in the P7 control, *Atoh1-Cre; Atoh1*$^{f/kiNeurog1}$ and *Atoh1-Cre; Atoh1*$^{f/f}$ mice in 300 µm stretches in comparable regions in the apex, middle and base of the cochlea after performing immunohistochemistry for Myo7a and tubulin. Quantification was performed in six independent cochleae from each genotype. For further details, see the supplementary Materials and Methods. The data obtained from the quantification of IHCs, OHCs and IP cells were analyzed using Student's *t*-test. $P<0.05$ was considered statistically significant.

Auditory brainstem response (ABR) recording

Following sedation, ABR recording was performed in 1-month-old control and *Atoh1-Cre; Atoh1*$^{f/kiNeurog1}$ littermate mice. A loudspeaker was placed 10 cm from the pinna of the test ear and computer-generated clicks were given in an open field environment in a soundproof chamber. Click responses were averaged and recorded signals were bandpass filtered (300 Hz-5 kHz) with a 60 Hz notch filter. The sound level was decreased in 10 dB steps from a 96 dB sound pressure level until there was no noticeable response. For further details, see the supplementary Materials and Methods.

Scanning electron microscopy (SEM)

SEM was performed as previously described (Jahan et al., 2012). A detailed description is provided in the supplementary Materials and Methods.

Acknowledgements

We thank Dr Fernando Giráldez for constructive and valuable comments on the manuscript; Qiufu Ma (*Neurog1*), Huda Y. Zoghbi (*Atoh1*), Mengqing Xiang (*Barhl1* and *Pou4f3*), Jacqueline E. Lee (*Neurod1*), Ulla Pirvola (*Fgf8*), Thomas Gridley (*Jag1*), Brigid L. M. Hogan (*Fgf10*), Doris K. Wu (*Bmp4*), Andy Groves (*Hes5*) and Guillermo Oliver (*Prox1*) for providing plasmids for *in situ* hybridization; the Central Microscopy Research Facility for carrying out SEM; the Roy J. Carver Center for Imaging for use of the Leica TCS SP5 confocal microscope; the Roy J. Carver Center for Genomics for use of the Roche 480 LightCycler; and the Iowa Center for Molecular Auditory Neuroscience (P30; ICMAN) for the use of the ABR facility at the University of Iowa.

Competing interests

The authors declare no competing or financial interests.

Author contributions

I.J., N.P. and B.F. conceived the work; N.P. and J.K. performed mouse breeding and genotyping; I.J. collected and analyzed the data; I.J. and B.F. wrote the paper.

Funding

This work was supported by the National Institute on Deafness and Other Communication Disorders (NIDCD) [R03 DC013655 to I.J.]; and the Hearing Health Foundation (Emerging Research Grant to I.J.). We thank the Office of the Vice President for Research (OVPR), University of Iowa College of Liberal Arts and Sciences (CLAS), and the P30 core grant for support [DC 010362]. The funders had no role in study design, data collection and analysis, decision to publish, or preparation of the manuscript. Deposited in PMC for release after 12 months.

Supplementary material

Supplementary material available online at
http://dev.biologists.org/lookup/suppl/doi:10.1242/dev.123091/-/DC1

References

Ahmed, M., Wong, E. Y. M., Sun, J., Xu, J., Wang, F. and Xu, P.-X. (2012). Eya1-Six1 interaction is sufficient to induce hair cell fate in the cochlea by activating Atoh1 expression in cooperation with Sox2. *Dev. Cell* **22**, 377-390.

Benito-Gonzalez, A. and Doetzlhofer, A. (2014). Hey1 and hey2 control the spatial and temporal pattern of mammalian auditory hair cell differentiation downstream of hedgehog signaling. *J. Neurosci.* **34**, 12865-12876.

Development (2015) 142, 2810-2821 doi:10.1242/dev.123091

Bermingham, N. A., Hassan, B. A., Price, S. D., Vollrath, M. A., Ben-Arie, N., Eatock, R. A., Bellen, H. J., Lysakowski, A. and Zoghbi, H. Y. (1999). Math1: an essential gene for the generation of inner ear hair cells. *Science* **284**, 1837-1841.

Brooker, R., Hozumi, K. and Lewis, J. (2006). Notch ligands with contrasting functions: Jagged1 and Delta1 in the mouse inner ear. *Development* **133**, 1277-1286.

Bustin, S. A., Benes, V., Garson, J. A., Hellemans, J., Huggett, J., Kubista, M., Mueller, R., Nolan, T., Pfaffl, M. W., Shipley, G. L. et al. (2009). The MIQE guidelines: minimum information for publication of quantitative real-time PCR experiments. *Clin. Chem.* **55**, 611-622.

Cai, H., Richter, C.-P. and Chadwick, R. S. (2003). Motion analysis in the hemicochlea. *Biophys. J.* **85**, 1929-1937.

Cai, T., Seymour, M. L., Zhang, H., Pereira, F. A. and Groves, A. K. (2013). Conditional deletion of Atoh1 reveals distinct critical periods for survival and function of hair cells in the organ of Corti. *J. Neurosci.* **33**, 10110-10122.

Cai, T., Jen, H.-I., Kang, H., Klisch, T. J., Zoghbi, H. Y. and Groves, A. K. (2015). Characterization of the transcriptome of nascent hair cells and identification of direct targets of the Atoh1 transcription factor. *J. Neurosci.* **35**, 5870-5883.

Chellappa, R., Li, S., Pauley, S., Jahan, I., Jin, K. and Xiang, M. (2008). Barhl1 regulatory sequences required for cell-specific gene expression and autoregulation in the inner ear and central nervous system. *Mol. Cell. Biol.* **28**, 1905-1914.

Chen, K. H., Boettiger, A. N., Moffitt, J. R., Wang, S. and Zhuang, X. (2015). Spatially resolved, highly multiplexed RNA profiling in single cells. *Science* **348**, aaa6090.

Chonko, K. T., Jahan, I., Stone, J., Wright, M. C., Fujiyama, T., Hoshino, M., Fritzsch, B. and Maricich, S. M. (2013). Atoh1 directs hair cell differentiation and survival in the late embryonic mouse inner ear. *Dev. Biol.* **381**, 401-410.

Doetzlhofer, A., Basch, M. L., Ohyama, T., Gessler, M., Groves, A. K. and Segil, N. (2009). Hey2 regulation by FGF provides a Notch-independent mechanism for maintaining pillar cell fate in the organ of Corti. *Dev. Cell* **16**, 58-69.

Driver, E. C., Sillers, L., Coate, T. M., Rose, M. F. and Kelley, M. W. (2013). The Atoh1-lineage gives rise to hair cells and supporting cells within the mammalian cochlea. *Dev. Biol.* **376**, 86-98.

Du, X., Jensen, P., Goldowitz, D. and Hamre, K. M. (2007). Wild-type cells rescue genotypically *Math1*-null hair cells in the inner ears of chimeric mice. *Dev. Biol.* **305**, 430-438.

Fritzsch, B., Matei, V. A., Nichols, D. H., Bermingham, N., Jones, K., Beisel, K. W. and Wang, V. Y. (2005). Atoh1 null mice show directed afferent fiber growth to undifferentiated ear sensory epithelia followed by incomplete fiber retention. *Dev. Dyn.* **233**, 570-583.

Fritzsch, B., Beisel, K. W. and Hansen, L. A. (2006). The molecular basis of neurosensory cell formation in ear development: a blueprint for hair cell and sensory neuron regeneration? *Bioessays* **28**, 1181-1193.

Fritzsch, B., Dillard, M., Lavado, A., Harvey, N. L. and Jahan, I. (2010a). Canal cristae growth and fiber extension to the outer hair cells of the mouse ear require Prox1 activity. *PLoS ONE* **5**, e9377.

Fritzsch, B., Eberl, D. F. and Beisel, K. W. (2010b). The role of bHLH genes in ear development and evolution: revisiting a 10-year-old hypothesis. *Cell. Mol. Life Sci.* **67**, 3089-3099.

Fritzsch, B., Jahan, I., Pan, N. and Elliott, K. (2014a). Evolving gene regulation networks into cellular networks guiding adaptive behavior: an outline how single cells could have evolved into a centralized neurosensory system. *Cell Tissue Res.* **378**, 1-19.

Fritzsch, B., Pan, N., Jahan, I. and Elliott, K. (2014b). Inner ear development: building a spiral ganglion and an organ of Corti out of unspecified ectoderm. *Cell Tissue Res.* **361**, 7-24.

Fritzsch, B., Jahan, I., Pan, N. and Elliott, K. L. (2015). Evolving gene regulatory networks into cellular networks guiding adaptive behavior: an outline how single cells could have evolved into a centralized neurosensory system. *Cell Tissue Res.* **359**, 295-313.

Groves, A. K. and Fekete, D. M. (2012). Shaping sound in space: the regulation of inner ear patterning. *Development* **139**, 245-257.

Guillemot, F. (2007). Spatial and temporal specification of neural fates by transcription factor codes. *Development* **134**, 3771-3780.

Helms, A. W., Abney, A. L., Ben-Arie, N., Zoghbi, H. Y. and Johnson, J. E. (2000). Autoregulation and multiple enhancers control Math1 expression in the developing nervous system. *Development* **127**, 1185-1196.

Hertzano, R., Montcouquiol, M., Rashi-Elkeles, S., Elkon, R., Yücel, R., Frankel, W. N., Rechavi, G., Möröy, T., Friedman, T. B., Kelley, M. W. et al. (2004). Transcription profiling of inner ears from Pou4f3ddl/ddl identifies Gfi1 as a target of the Pou4f3 deafness gene. *Hum. Mol. Genet.* **13**, 2143-2153.

Hertzano, R., Shalit, E., Rzadzinska, A. K., Dror, A. A., Song, L., Ron, U., Tan, J. T., Shitrit, A. S., Fuchs, H., Hasson, T. et al. (2008). A Myo6 mutation destroys coordination between the myosin heads, revealing new functions of myosin VI in the stereocilia of mammalian inner ear hair cells. *PLoS Genet.* **4**, e1000207.

Hudspeth, A. (2014). Integrating the active process of hair cells with cochlear function. *Nat. Rev. Neurosci.* **15**, 600-614.

Huh, S.-H., Jones, J., Warchol, M. E. and Ornitz, D. M. (2012). Differentiation of the lateral compartment of the cochlea requires a temporally restricted FGF20 signal. *PLoS Biol.* **10**, e1001231.

Imayoshi, I. and Kageyama, R. (2014). bHLH factors in self-renewal, multipotency, and fate choice of neural progenitor cells. *Neuron* **82**, 9-23.

Jacobo, A. and Hudspeth, A. (2014). Reaction–diffusion model of hair-bundle morphogenesis. *Proc. Natl. Acad. Sci. USA* **111**, 15444-15449.

Jacques, B. E., Montcouquiol, M. E., Layman, E. M., Lewandoski, M. and Kelley, M. W. (2007). Fgf8 induces pillar cell fate and regulates cellular patterning in the mammalian cochlea. *Development* **134**, 3021-3029.

Jahan, I., Pan, N., Kersigo, J. and Fritzsch, B. (2010). Neurod1 suppresses hair cell differentiation in ear ganglia and regulates hair cell subtype development in the cochlea. *PLoS ONE* **5**, e11661.

Jahan, I., Pan, N., Kersigo, J., Calisto, L. E., Morris, K. A., Kopecky, B., Duncan, J. S., Beisel, K. W. and Fritzsch, B. (2012). Expression of Neurog1 instead of Atoh1 can partially rescue organ of Corti cell survival. *PLoS ONE* **7**, e30853.

Jahan, I., Pan, N., Kersigo, J. and Fritzsch, B. (2013). Beyond generalized hair cells: molecular cues for hair cell types. *Hear. Res.* **297**, 30-41.

Jahan, I., Pan, N., Elliott, K. L. and Fritzsch, B. (2015). The quest for restoring hearing: understanding ear development more completely. *Bioessays* **37**, 1-12.

Johnston, R. J., Jr and Desplan, C. (2014). Interchromosomal communication coordinates intrinsically stochastic expression between alleles. *Science* **343**, 661-665.

Kelly, M. C., Chang, Q., Pan, A., Lin, X. and Chen, P. (2012). Atoh1 directs the formation of sensory mosaics and induces cell proliferation in the postnatal mammalian cochlea in vivo. *J. Neurosci.* **32**, 6699-6710.

Kersigo, J. and Fritzsch, B. (2015). Inner ear hair cells deteriorate in mice engineered to have no or diminished innervation. *Front. Aging Neurosci.* **7**, 33.

Kiernan, A. E., Xu, J. and Gridley, T. (2006). The Notch ligand JAG1 is required for sensory progenitor development in the mammalian inner ear. *PLoS Genet.* **2**, e4.

Kitajiri, S.-I., Sakamoto, T., Belyantseva, I. A., Goodyear, R. J., Stepanyan, R., Fujiwara, I., Bird, J. E., Riazuddin, S., Riazuddin, S., Ahmed, Z. M. et al. (2010). Actin-bundling protein TRIOBP forms resilient rootlets of hair cell stereocilia essential for hearing. *Cell* **141**, 786-798.

Kobayashi, T. and Kageyama, R. (2014). Expression dynamics and functions of Hes factors in development and diseases. *Curr. Top. Dev. Biol.* **110**, 263-283.

Kuhn, S., Johnson, S. L., Furness, D. N., Chen, J., Ingham, N., Hilton, J. M., Steffes, G., Lewis, M. A., Zampini, V., Hackney, C. M. et al. (2011). miR-96 regulates the progression of differentiation in mammalian cochlear inner and outer hair cells. *Proc. Natl. Acad. Sci. USA* **108**, 2355-2360.

Lee, S., Danielian, P. S., Fritzsch, B. and McMahon, A. P. (1997). Evidence that FGF8 signalling from the midbrain-hindbrain junction regulates growth and polarity in the developing midbrain. *Development* **124**, 959-969.

Lewis, M. A., Quint, E., Glazier, A. M., Fuchs, H., De Angelis, M. H., Langford, C., van Dongen, S., Abreu-Goodger, C., Piipari, M., Redshaw, N. et al. (2009). An ENU-induced mutation of miR-96 associated with progressive hearing loss in mice. *Nat. Genet.* **41**, 614-618.

Li, S., Price, S. M., Cahill, H., Ryugo, D. K., Shen, M. M. and Xiang, M. (2002). Hearing loss caused by progressive degeneration of cochlear hair cells in mice deficient for the Barhl1 homeobox gene. *Development* **129**, 3523-3532.

Ma, Q., Anderson, D. J. and Fritzsch, B. (2000). Neurogenin 1 null mutant ears develop fewer, morphologically normal hair cells in smaller sensory epithelia devoid of innervation. *J. Assoc. Res. Otolaryngol.* **1**, 129-143.

Mao, C.-A., Wang, S. W., Pan, P. and Klein, W. H. (2008). Rewiring the retinal ganglion cell gene regulatory network: Neurod1 promotes retinal ganglion cell fate in the absence of Math5. *Development* **135**, 3379-3388.

Mao, C.-A., Cho, J.-H., Wang, J., Gao, Z., Pan, P., Tsai, W.-W., Frishman, L. J. and Klein, W. H. (2013). Reprogramming amacrine and photoreceptor progenitors into retinal ganglion cells by replacing Neurod1 with Atoh7. *Development* **140**, 541-551.

Masuda, M., Pak, K., Chavez, E. and Ryan, A. F. (2012). TFE2 and GATA3 enhance induction of POU4F3 and myosin VIIa positive cells in nonsensory cochlear epithelium by ATOH1. *Dev. Biol.* **372**, 68-80.

Matei, V., Pauley, S., Kaing, S., Rowitch, D., Beisel, K. W., Morris, K., Feng, F., Jones, K., Lee, J. and Fritzsch, B. (2005). Smaller inner ear sensory epithelia in Neurog 1 null mice are related to earlier hair cell cycle exit. *Dev. Dyn.* **234**, 633-650.

Mizutari, K., Fujioka, M., Hosoya, M., Bramhall, N., Okano, H. J., Okano, H. and Edge, A. S. B. (2013). Notch inhibition induces cochlear hair cell regeneration and recovery of hearing after acoustic trauma. *Neuron* **77**, 58-69.

Mogensen, M. M., Rzadzinska, A. and Steel, K. P. (2007). The deaf mouse mutant whirler suggests a role for whirlin in actin filament dynamics and stereocilia development. *Cell Motil. Cytoskeleton* **64**, 496-508.

Mueller, K. L., Jacques, B. E. and Kelley, M. W. (2002). Fibroblast growth factor signaling regulates pillar cell development in the organ of corti. *J. Neurosci.* **22**, 9368-9377.

Müller, U. and Barr-Gillespie, P. G. (2015). New treatment options for hearing loss. *Nat. Rev. Drug Discov.* **14**, 346-365.

Pan, N., Jahan, I., Lee, J. E. and Fritzsch, B. (2009). Defects in the cerebella of conditional Neurod1 null mice correlate with effective Tg(Atoh1-cre)

recombination and granule cell requirements for Neurod1 for differentiation. *Cell Tissue Res.* **337**, 407-428.

Pan, N., Jahan, I., Kersigo, J., Kopecky, B., Santi, P., Johnson, S., Schmitz, H. and Fritzsch, B. (2011). Conditional deletion of Atoh1 using Pax2-Cre results in viable mice without differentiated cochlear hair cells that have lost most of the organ of Corti. *Hear. Res.* **275**, 66-80.

Pan, N., Jahan, I., Kersigo, J., Duncan, J. S., Kopecky, B. and Fritzsch, B. (2012a). A novel Atoh1 "self-terminating" mouse model reveals the necessity of proper Atoh1 level and duration for hair cell differentiation and viability. *PLoS ONE* **7**, e30358.

Pan, N., Kopecky, B., Jahan, I. and Fritzsch, B. (2012b). Understanding the evolution and development of neurosensory transcription factors of the ear to enhance therapeutic translation. *Cell Tissue Res.* **349**, 415-432.

Perrin, B. J., Sonnemann, K. J. and Ervasti, J. M. (2010). β-actin and γ-actin are each dispensable for auditory hair cell development but required for stereocilia maintenance. *PLoS Genet.* **6**, e1001158.

Petrovic, J., Galvez, H., Neves, J., Abello, G. and Giraldez, F. (2015). Differential regulation of Hes/Hey genes during inner ear development. *Dev. Neurobiol.* **75**, 703-720.

Pirvola, U., Spencer-Dene, B., Xing-Qun, L., Kettunen, P., Thesleff, I., Fritzsch, B., Dickson, C. and Ylikoski, J. (2000). FGF/FGFR-2 (IIIb) signaling is essential for inner ear morphogenesis. *J. Neurosci.* **20**, 6125-6134.

Raft, S., Koundakjian, E. J., Quinones, H., Jayasena, C. S., Goodrich, L. V., Johnson, J. E., Segil, N. and Groves, A. K. (2007). Cross-regulation of Ngn1 and Math1 coordinates the production of neurons and sensory hair cells during inner ear development. *Development* **134**, 4405-4415.

Reiprich, S. and Wegner, M. (2015). From CNS stem cells to neurons and glia: sox for everyone. *Cell Tissue Res.* **359**, 111-124.

Ronaghi, M., Nasr, M., Ealy, M., Durruthy-Durruthy, R., Waldhaus, J., Diaz, G. H., Joubert, L.-M., Oshima, K. and Heller, S. (2014). Inner ear hair cell-like cells from human embryonic stem cells. *Stem Cells Dev.* **23**, 1275-1284.

Rzadzinska, A. K., Nevalainen, E. M., Prosser, H. M., Lappalainen, P. and Steel, K. P. (2009). MyosinVIIa interacts with Twinfilin-2 at the tips of mechanosensory stereocilia in the inner ear. *PLoS ONE* **4**, e7097.

Schwander, M., Kachar, B. and Müller, U. (2010). Review series: the cell biology of hearing. *J. Cell Biol.* **190**, 9-20.

Sekerková, G., Richter, C.-P. and Bartles, J. R. (2011). Roles of the espin actin-bundling proteins in the morphogenesis and stabilization of hair cell stereocilia revealed in CBA/CaJ congenic jerker mice. *PLoS Genet.* **7**, e1002032.

Self, T., Mahony, M., Fleming, J., Walsh, J., Brown, S. and Steel, K. P. (1998). Shaker-1 mutations reveal roles for myosin VIIA in both development and function of cochlear hair cells. *Development* **125**, 557-566.

Self, T., Sobe, T., Copeland, N. G., Jenkins, N. A., Avraham, K. B. and Steel, K. P. (1999). Role of myosin VI in the differentiation of cochlear hair cells. *Dev. Biol.* **214**, 331-341.

Sheykholeslami, K., Thimmappa, V., Nava, C., Bai, X., Yu, H., Zheng, T., Zhang, Z., Li, S. L., Liu, S. and Zheng, Q. Y. (2013). A new mutation of the Atoh1 gene in mice with normal life span allows analysis of inner ear and cerebellar phenotype in aging. *PLoS ONE* **8**, e79791.

Sienknecht, U. J., Köppl, C. and Fritzsch, B. (2014). Evolution and development of hair cell polarity and efferent function in the inner ear. *Brain Behav. Evol.* **83**, 150-161.

Slepecky, N. B. (1996). Structure of the mammalian cochlea. In *The cochlea*, pp. 44-129. New York: Springer.

Sprinzak, D., Lakhanpal, A., LeBon, L., Garcia-Ojalvo, J. and Elowitz, M. B. (2011). Mutual inactivation of Notch receptors and ligands facilitates developmental patterning. *PLoS Comput. Biol.* **7**, e1002069.

Tan, J., Clarke, M., Barrett, G. and Millard, R. (2010). The p75 neurotrophin receptor protects primary auditory neurons against acoustic trauma in mice. *Hear. Res.* **268**, 46-59.

Taylor, R., Bullen, A., Johnson, S. L., Grimm-Günter, E.-M., Rivero, F., Marcotti, W., Forge, A. and Daudet, N. (2015). Absence of plastin 1 causes abnormal maintenance of hair cell stereocilia and a moderate form of hearing loss in mice. *Hum. Mol. Genet.* **24**, 37-49.

Ueyama, T., Sakaguchi, H., Nakamura, T., Goto, A., Morioka, S., Shimizu, A., Nakao, K., Hishikawa, Y., Ninoyu, Y., Kassai, H. et al. (2014). Maintenance of stereocilia and apical junctional complexes by Cdc42 in cochlear hair cells. *J. Cell Sci.* **127**, 2040-2052.

von Bartheld, C. S., Patterson, S. L., Heuer, J. G., Wheeler, E. F., Bothwell, M. and Rubel, E. W. (1991). Expression of nerve growth factor (NGF) receptors in the developing inner ear of chick and rat. *Development* **113**, 455-470.

Wang, V. Y., Hassan, B. A., Bellen, H. J. and Zoghbi, H. Y. (2002). Drosophila atonal fully rescues the phenotype of Math1 null mice: new functions evolve in new cellular contexts. *Curr. Biol.* **12**, 1611-1616.

Weston, M. D., Pierce, M. L., Jensen-Smith, H. C., Fritzsch, B., Rocha-Sanchez, S., Beisel, K. W. and Soukup, G. A. (2011). MicroRNA-183 family expression in hair cell development and requirement of microRNAs for hair cell maintenance and survival. *Dev. Dyn.* **240**, 808-819.

Xiang, M., Maklad, A., Pirvola, U. and Fritzsch, B. (2003). Brn3c null mutant mice show long-term, incomplete retention of some afferent inner ear innervation. *BMC Neurosci.* **4**, 2.

Yamamoto, S., Schulze, K. L. and Bellen, H. J. (2014). Introduction to Notch signaling. In *Notch Signaling*, pp. 1-14. New York: Springer.

Yang, S.-M., Chen, W., Guo, W.-W., Jia, S., Sun, J.-H., Liu, H.-Z., Young, W.-Y. and He, D. Z. Z. (2012). Regeneration of stereocilia of hair cells by forced Atoh1 expression in the adult mammalian cochlea. *PLoS ONE* **7**, e46355.

Zheng, J. L. and Gao, W.-Q. (2000). Overexpression of Math1 induces robust production of extra hair cells in postnatal rat inner ears. *Nat. Neurosci.* **3**, 580-586.

Zine, A. and de Ribaupierre, F. (2002). Notch/Notch ligands and Math1 expression patterns in the organ of Corti of wild-type and Hes1 and Hes5 mutant mice. *Hear. Res.* **170**, 22-31.

Zine, A., Aubert, A., Qiu, J., Therianos, S., Guillemot, F., Kageyama, R. and de Ribaupierre, F. (2001). Hes1 and Hes5 activities are required for the normal development of the hair cells in the mammalian inner ear. *J. Neurosci.* **21**, 4712-4720.

Zine, A., Löwenheim, H. and Fritzsch, B. (2014). Toward translating molecular ear development to generate hair cells from stem cells. In *Adult Stem Cells*, pp. 111-161. New York: Springer.

Supporting Information:

Supplementary Figures:

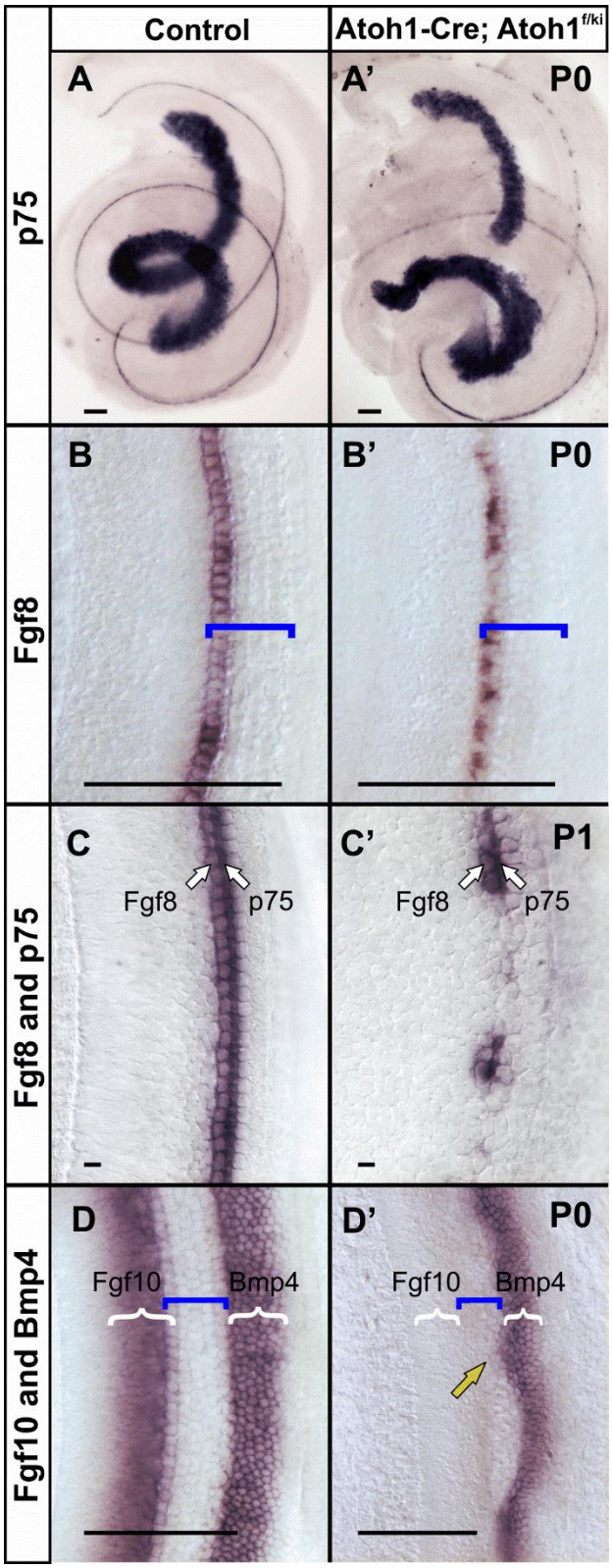

Figure S1. ***Fgf8* expression loss correlates with the *p75* expression loss and *Fgf10* and *Bmp4* are changed.** ISH of p75 reveals expression in the IP cells with a gradient from apex to base of the cochlea in the P0 *Atoh1-Cre; Atoh1*$^{f/kiNeurog1}$ mice (A, A'). *Fgf8* expression is also reduced in the IHC in the P0 *Atoh1-Cre; Atoh1*$^{f/kiNeurog1}$ mice (B, B'). Double ISH of *p75* and *Fgf8* in the P1 cochlea reveal that the loss of *Fgf8* expressing IHC correlates with the loss of *p75* positive IP cells (C,C'). Double ISH of *Fgf10* and *Bmp4* shows that *Fgf10* is nearly eliminated and *Bmp4* flanking the lateral/abneural boundary of the OC shows medial expansion in the *Atoh1-Cre; Atoh1*$^{f/kiNeurog1}$ mice (D, yellow arrow in D') like self-terminating mice (Pan et al., 2012a). Bar indicates 100 μm in all except 10 μm in C,C'.

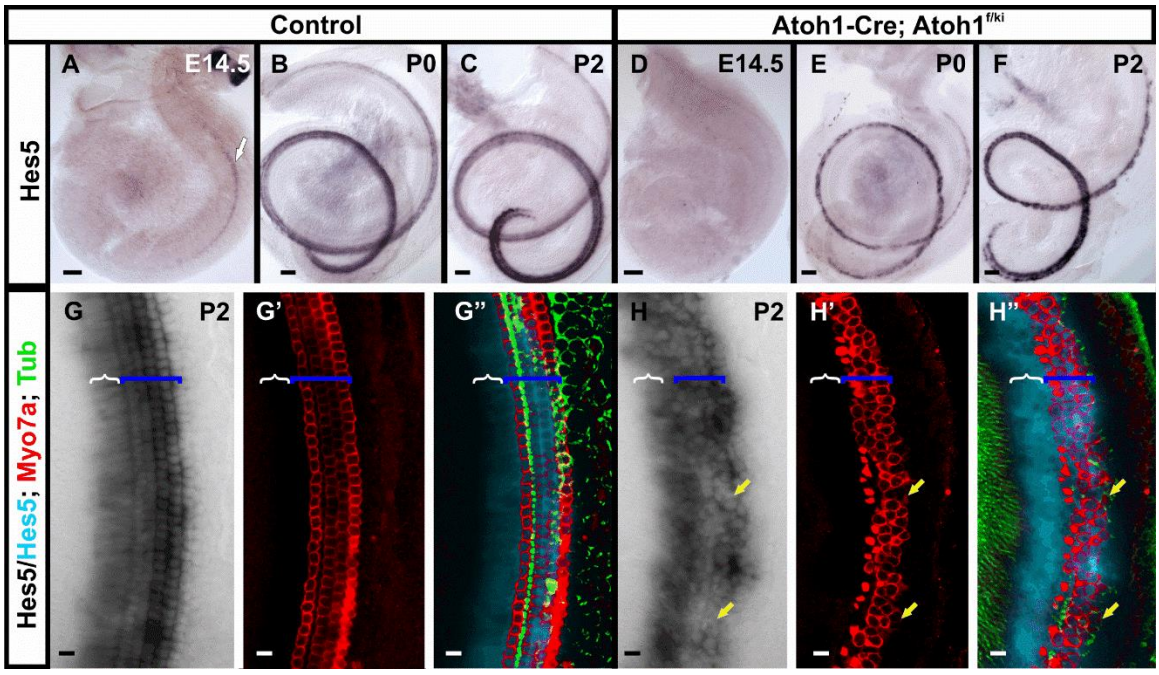

Figure S2. **Aberration of *Hes5* expression in the *Atoh1-Cre; Atoh1*$^{f/kiNeurog1}$ mice.** *Hes5* is upregulated in the mid-base of the control cochlea at E14.5 (A). *Hes5* is delayed in the littermate *Atoh1-Cre; Atoh1*$^{f/kiNeurog1}$ cochlea (D) that is upregulated later at P0 and P2 (E, F). *Hes5*, is dominantly expressed in the lateral SCs in the P2 control mice (G). In the *Atoh1-Cre; Atoh1*$^{f/kiNeurog1}$ mice, *Hes5* is differentially downregulated, particularly toward the base. Myo7a and Tubulin immunohistochemistry in the *Hes5* ISH reacted cochlea reveals that patchy downregulation of *Hes5* in *Atoh1-Cre; Atoh1*$^{f/kiNeurog1}$ mice is not associated with the quantitative changes of HCs (arrows in H-H") as reported in *Hes5* deletion mutants (Zine et al., 2001; Zine and de Ribaupierre, 2002). We use a false cyan color to show the ISH stain while combined with the immunohistochemistry. '{'demarcates the expression of *Hes5* in the GER and '[' in the OC. Bar indicates 100 µm in A-F and 10 µm in G-H".

Supplementary Tables:

Table S1. Total length measurement of the cochlea at P7. The total lengths of the cochleae at P7 display no substantial difference in both *Atoh1-Cre; Atoh1$^{f/kiNeurog1}$* and *Atoh1-Cre; Atoh1$^{f/f}$* mice compared to control littermates.

Total Length in µm	**Control**	***Atoh1-Cre; Atoh1$^{f/ki}$***	***Atoh1-Cre; Atoh1$^{f/f}$***
Mean (N=3)	6561±497	6523±187	6459±288

Table S2. The quantification of HCs and IP cells in the equivalent segments of the control, *Atoh1-Cre; Atoh1$^{f/kiNeurog1}$* and *Atoh1-Cre; Atoh1$^{f/f}$* cochlea at P7.

Mean of IHCs count (N=6)	**Control**	***Atoh1-Cre; Atoh1$^{f/ki}$***	***Atoh1-Cre; Atoh1$^{f/f}$***
Apex	37±1	33±8	10±1
Middle	40±1	42±5	18±4
Base	33±3	33±4	20±5
Mean of OHCs count	Control	*Atoh1-Cre; Atoh1$^{f/ki}$*	*Atoh1-Cre; Atoh1$^{f/f}$*
Apex	127±3	96±25	63±10
Middle	129±4	71±17	41±8
Base	115±6	64±16	28±13
Mean of IP cells count	Control	*Atoh1-Cre; Atoh1$^{f/ki}$*	*Atoh1-Cre; Atoh1$^{f/f}$*
Apex	53±6	45±4	34±6
Middle	59±3	42±3	28±5
Base	51±8	43±7	21±6

Table S3. Primer sequences used for the RT-qPCR are shown here.

Name	**Accession number**	**Primer Sequence**	**In silico Tm**	**% GC**	**Amplicon Length (bp)**
Neurog1	NM_010896.2	**Forward**: ggcctttgtaaggcaacatc **Reverse:** cagccagttccccatctatt	59/59	50/50	73
Pou4f3	NM_138945.2	**Forward**: ccccgtactgcaagaacc **Reverse:** catcaaagcttccaaatatattaccc	59/60	61/35	113
Barhl1	NM_019446.4	**Forward**: ggtaccagaaccgcagga **Reverse:** tggagcgccgagtaattg	59/60	61/56	88
Actb	NM_007393.3	**Forward**: ctaaggccaaccgtgaaaag **Reverse:** accagaggcatacagggaca	59/60	50/55	104

Supplementary Materials and Methods:

Genotyping

EconoTaq plus green 2X master mix (Lucigen, 30033) and a three primer sets were used for the genotyping of tail DNA. All resultant products were electrophoresed and visualized on a 2% agarose gel. The different primer sets were used to detect *Atoh1* floxed allele, *Atoh1*^{kiNeurog1} allele and *Cre*-specific primers to detect *Atoh1-Cre* transgene as described (Jahan et al., 2012; Pan et al., 2012a).

In situ hybridization

For *in situ* hybridization, the plasmids containing the cDNAs were used to generate the RNA probe by *in vitro* transcription. After being anesthetized with 2,2,2 tribromoethanol (Avertin), mice were perfused in 4% paraformaldehyde (PFA) and fixed overnight in 4% PFA. The ears were dissected in 0.4% PFA and dehydrated and rehydrated in graded methanol series and then digested briefly with 20 µg/ml of Proteinase K (Ambion, Austin, TX, USA) for 15-20 minutes. The samples were then hybridized overnight at 60°C to the riboprobe in hybridization solution. The samples were incubated overnight with an anti-digoxigenin antibody after washing off the unbound probe (Roche Diagnostics GmbH, Mannheim, Germany). After a series of washes, the samples were reacted with nitroblue phosphate/ 5-bromo, 4-chloro, 3-indolil phosphate (BM purple substrate, Roche Diagnostics, Germany) which is enzymatically converted to a purple colored product. The ears were mounted flat in glycerol and viewed in a Nikon Eclipse 800 microscope using differential interference contrast microscopy and images were captured with Metamorph software. The ears of the littermate of different genotype for the same gene expression were performed in the same reaction tubes to maintain the reaction accuracy.

Immunohistochemistry

For immunohistochemistry, decalcification was performed by incubating the postnatal ears in EDTA in 0.4% PFA before the microdissection. Then the ears were dehydrated in 100% ethanol and rehydrated in graded ethanol series and then washed in PBS and blocked with 2.5% normal goat serum in PBS containing 0.5% Triton-X-100 for 1 hour. Then the ears were incubated in

primary antibodies for Myo7a (Myosin 7a, Proteus Biosciences), tubulin (Sigma) and p75 (Sigma) in dilutions of 1:200, 1:800 and 1:1000 respectively for 24-48 hours at 4˚C. After several washes with PBS, corresponding secondary antibodies (1:500) (Alexa fluor molecular probe 647 or 532 or 488; Invitrogen) were added and incubated overnight at 4°C. Hoechst nuclear stain (Polysciences; 10mg/ml) was used at a dilution of 1:1000 at room temperature for 1 hour. The ears were washed with PBS and mounted in glycerol and images were taken with a Leica TCS SP5 confocal microscope.

Cell Counts

IHCs, OHCs and IP cells were counted in the comparable regions of P7 control, *Atoh1-Cre; Atoh1*$^{f/kiNeurog1}$ and *Atoh1-Cre; Atoh1*$^{f/f}$ cochleae after performing the immunohistochemistry of Myo7a and tubulin. Each cochlea was divided into 3 equal segments as apex, middle and base and the overview images (100x magnification) were taken to select the area for quantification. 10% distant from the apical tip was chosen for 'apex', 50% for 'Mid' and 90% for the 'base' quantification. Counting was performed on enlarged images at the 400x magnification in SP5 confocal microscope using the LIF software in the 300 µm stretch of apex, middle and base of the cochleae. LIF software allows computerized number markings after each count to facilitate accurate quantification. Tubulin positive IP cells were used to demarcate IHCs as medial to IP cells and OHCs as lateral to the IP cells.

Auditory brainstem response (ABR) recording

2,2,2 tribromoethanol (0.025 ml/g of body weight) was injected in one month old control and *Atoh1-Cre; Atoh1*$^{f/kiNeurog1}$ littermate mice and absence of ocular and pedal reflexes were assessed for surgical level of anesthesia. Needle electrodes were then inserted subcutaneously in the vertex, slightly posterior to the pinna and in the contralateral hind limb. A loudspeaker was placed 10 cm away from the pinna of the test ear and computer-generated clicks were given in an open field environment in a soundproof chamber. Click responses were averaged across 512 presentations using Tucker-Davis Technologies System hardware running BioSig® Software. Recorded signals were bandpass filtered (300 Hz–5 kHz) and 60Hz notch filter. The sound level was decreased in 10-dB steps from a 96-dB sound pressure level until there was no noticeable response.

Scanning electron microscopy (SEM)

The mice for SEM were perfused and fixed in 2.5% gluteraldehyde in 1% PFA after sedating with 2,2,2 tribromoethanol. Ears of postnatal mice were decalcified with EDTA. Following osmication in 2% osmium tetroxide in 0.1 M phosphate buffer (pH 7.4) for up to 1 hour, the ears were microdissected including removal of the Reissners membrane and the tectorial membrane. The samples were then washed several times with distilled water to remove ions, dehydrated in a graded ethanol series, critical point dried, mounted on stubs and coated with gold/palladium. Stubs were viewed with a Hitachi S-4800 Scanning Electron Microscope with 3MeV acceleration.